NASA/TM–2022-219027/ Vol. 10

PACE Technical Report Series, Volume 10

Editors: Ivona Cetinić, Charles R. McClain, P. Jeremy Werdell, and Michael Behrenfeld

ACE Ocean Product Accuracy Assessments: A record of the state of the art circa 2010

NASA ACE Ocean Field and Laboratory Measurement Group

March 2022

NASA STI Program ... in Profile

Since its founding, NASA has been dedicated to the advancement of aeronautics and space science. The NASA scientific and technical information (STI) program plays a key part in helping NASA maintain this important role.

The NASA STI program operates under the auspices of the Agency Chief Information Officer. It collects, organizes, provides for archiving, and disseminates NASA's STI. The NASA STI program provides access to the NTRS Registered and its public interface, the NASA Technical Reports Server, thus providing one of the largest collections of aeronautical and space science STI in the world. Results are published in both non-NASA channels and by NASA in the NASA STI Report Series, which includes the following report types:

- TECHNICAL PUBLICATION. Reports of completed research or a major significant phase of research that present the results of NASA Programs and include extensive data or theoretical analysis. Includes compilations of significant scientific and technical data and information deemed to be of continuing reference value. NASA counterpart of peer-reviewed formal professional papers but has less stringent limitations on manuscript length and extent of graphic presentations.

- TECHNICAL MEMORANDUM. Scientific and technical findings that are preliminary or of specialized interest, e.g., quick release reports, working papers, and bibliographies that contain minimal annotation. Does not contain extensive analysis.

- CONTRACTOR REPORT. Scientific and technical findings by NASA-sponsored contractors and grantees.

- CONFERENCE PUBLICATION. Collected papers from scientific and technical conferences, symposia, seminars, or other meetings sponsored or co-sponsored by NASA.

- SPECIAL PUBLICATION. Scientific, technical, or historical information from NASA programs, projects, and missions, often concerned with subjects having substantial public interest.

- TECHNICAL TRANSLATION. English-language translations of foreign scientific and technical material pertinent to NASA's mission.

Specialized services also include organizing and publishing research results, distributing specialized research announcements and feeds, providing information desk and personal search support, and enabling data exchange services.

For more information about the NASA STI program, see the following:

- Access the NASA STI program home page at http://www.sti.nasa.gov

- E-mail your question to help@sti.nasa.gov

- Phone the NASA STI Information Desk at 757-864-9658

- Write to:
  NASA STI Information Desk
  Mail Stop 148
  NASA Langley Research Center
  Hampton, VA 23681-2199

NASA/TM–2022-219027/ Vol. 10

PACE Technical Report Series, Volume 10

Editors:

Ivona Cetinić
GESTAR II/Morgan State University, Baltimore, MD

Charles R. McClain
Science Applications International Corporation, McLean, VA

P. Jeremy Werdell
NASA Goddard Space Flight Center, Greenbelt, MD

Michael Behrenfeld
Oregon State University, Corvallis, OR

ACE Ocean Product Accuracy Assessments: A record of the state of the art circa 2010

NASA ACE Ocean Field and Laboratory Measurement Group

National Aeronautics and
Space Administration

Goddard Space Flight Center
Greenbelt, Maryland 20771

March 2022

Level of Review: This material has been technically reviewed by technical management.

Available from

NASA STI Program
Mail Stop 148
NASA's Langley Research
Center Hampton, VA
23681-2199

National Technical Information
Service 5285 Port Royal Road
Springfield, VA 22161
703-605-6000

Preface

In response to the National Research Council of the National Academy of Science Decadal Survey recommendations on future NASA Earth science missions (NRC 2007), the Aerosol, Cloud, ocean Ecology (ACE) formulation team was organized in 2008. The initial team consisted of three working groups representing the aerosol, cloud and ocean biology communities with a fourth subsequently added for ocean-aerosol interactions. To outline the requirements for ACE, each working group developed a Science Traceability Matrix (STM) illustrating the flow down from key science questions, to approaches for addressing these questions, to measurement (radiometric, geophysical, biogeochemical, ancillary) and mission support requirements (e.g., spacecraft attributes, ground system capabilities). Figure 1 is the STM produced by the ocean working group. This STM was the precursor of the PACE STM published in the PACE Science Definition Team Report (PACE Science Definition Team 2018). To define the sensor, spacecraft and support system configurations and costs, a number of instrument and mission design studies were conducted at the NASA Goddard Space Flight Center and the Jet Propulsion Laboratory. Eventually, it was decided that the active (aerosol lidar, dual-frequency cloud radar) and passive (ocean radiometer, polarimeter – note that four additional complementary cloud sensors were also considered) sensors could be flown on separate platforms because the passive sensors were technologically more mature and would be expected to have longer lifespans than the active sensors that could be launched later and still overlap the passive sensors.

Because the ocean product suite was relatively extensive and included both radiometric and biogeochemical quantities, the question was raised as to what accuracies were required to address the science questions. The limits to what the accuracies could be for a satellite mission are determined by the accuracies of the field and laboratory measurements and associated analysis methods. Although many targeted ACE ocean products were already being generated by operational missions like SeaWiFS and MODIS (acronyms expanded below), the community had never untaken a comprehensive assessment of the actual accuracies of relevant laboratory and field techniques that encompass all the products. Early in the SeaWiFS program, field measurement protocols were published to help ensure consistency in the data sets being collected for algorithm development and post-launch science product validation. These protocols were subsequently updated under the SIMBIOS project. Similarly, a series of pigment and radiometer calibration round-robins (SeaHARRE for pigments, SIRREX for radiometry) were initiated under the SeaWiFS project and continued under SIMBIOS as chlorophyll-a and water-leaving radiance or reflectance were viewed as the critical “climate quality” research products at the time. None of the other derived products had been given similar attention due to resource (funding and manpower) limitations.

Given the aforestated need, an assessment was conducted between the summer 2010 and the spring 2011 of the accuracies of field and laboratory measurement technologies and techniques associated with all of the derived products considered essential for addressing the key ACE ocean science questions. Members of the ACE ocean working group and others in the ocean biogeochemical community drafted the assessments and these were shared for comment and discussion during routine teleconferences. While the recommended satellite product ranges of values (baseline and threshold) were published in the PACE SDT report (its Table A.1), the actual collection of assessments was never published. Accordingly, these assessments are being provided here in this NASA PACE technical memorandum to serve as a reference

to what the state of the art was during the early phase of the ACE mission formulation which eventually evolved into the PACE mission.

Charles McClain

Retired, NASA Goddard Space Flight Center

Michael Behrenfeld

Oregon State University

National Research Council (NRC) of the National Academies (2007), Earth Science and Applications from Space: National Imperatives for the Next Decade and Beyond Chapter, The National Academies Press, Washington, D.C.

PACE Science Definition Team, *Pre-Aerosol, Clouds, and ocean Ecosystem (PACE) Mission Science Definition Team Report*, NASA T/M 2018-291026 Vol. 2, 274 pp., 2018.

Acronyms undefined in text

SeaWiFS	Sea-viewing Wide Field of View Sensor
MODIS	Moderate Resolution Imaging Spectroradiometer
SeaHARRE	SeaWiFS HPLC Round-Robin Experiment
SIRREX	SeaWiFS Intercalibration Round-Robin Experiment
SIMBIOS	Sensor Intercomparison and Merger for Biological and Interdisciplinary Oceanic Studies

Figure 1: ACE Ocean Ecosystem science traceability matrix (STM) linking focused science questions to observational and modeling requirements.

Category	Focused Questions*	Approach	Maps to Science Question	Measurement Requirements	Instrument Requirements	Platform Requir'ts	Other Needs
Ocean Biology	1 What are the standing stocks, composition, & productivity of ocean ecosystems? How and why are they changing? [OBB1] 2 How and why are ocean biogeochemical cycles changing? How do they influence the Earth system? [OBB2] 3 What are the material exchanges between land & ocean? How do they influence coastal ecosystems, biogeochemistry & habitats? How are they changing? [OBB1,2,3] 4 How do aerosols & clouds influence ocean ecosystems & biogeochemical cycles? How do ocean biological & photochemical processes affect the atmosphere and Earth system? [OBB2] 5 How do physical ocean processes affect ocean ecosystems & biogeochemistry? How do ocean biological processes influence ocean physics? [OBB1,2] 6 What is the distribution of algal blooms and their relation to harmful algal and eutrophication events? How are these events changing? [OBB1,4]	Quantify phytoplankton biomass, pigments, optical properties, key groups (functional/HABS), and productivity using bio-optical models & chlorophyll fluorescence	1 2 6	Water-leaving radiances in near-ultraviolet, visible, & near-infrared for separation of absorbing & scattering constituents and calculation of chlorophyll fluorescence Total radiances in UV, NIR, and SWIR for atmospheric corrections Cloud radiances for assessing instrument stray light	**Ocean Radiometer** • 5 nm resolution 350 to 755 nm ▷ 1000 – 1500 SNR for 15 nm aggregate bands UV & visible and 10 nm fluorescence bands (665, 678, 710, 748 nm centers) ▷ 10 to 40 nm width atmospheric correction bands at 748, 765, 820, 865, 1245, 1640, 2135 nm • 0.1% radiometric temporal stability (1 month demonstrated prelaunch) • 58.3° cross track scanning • Sensor tilt (±20°) for glint avoidance • Polarization insensitive (<1.0%) • 1 km spatial resolution @ nadir • No saturation in UV to NIR bands • 5 year minimum design lifetime	Orbit permitting 2-day global coverage of ocean radiometer measurements Sun-synchronous orbit with crossing time between 10:30 a.m. & 1:30 p.m. Storage and download of full spectral and spatial data Monthly lunar calibration at 7° phase angle through Earth observing port	Global data sets from missions, models, or field observations: *Measurement Requirements* (1) Ozone (2) Total water vapor (3) Surface wind velocity (4) Surface barometric pressure (5) NO_2 concentration (6) Vicarious calibration & validation** (7) Full prelaunch characterization (2% accuracy radiometric) *Science Requirements* (1) SST (2) SSH (3) PAR (4) UV (5) MLD (6) CO_2 (7) pH (8) Ocean circulation (9) Aerosol deposition (10) run-off loading in coastal zone
		Measure particulate and dissolved carbon pools, their characteristics and optical properties	2 3				
		Quantify ocean photobiochemical & photobiological processes	2 4				
		Estimate particle abundance, size distribution (PSD), & characteristics	1 3 2				
		Assimilate ACE observations in ocean biogeochemical model fields of key properties (cf., air-sea CO_2 fluxes, export, pH, etc.)	2	High vertical resolution aerosol heights, optical thickness, & composition for atmospheric corrections Subsurface particle scattering & depth profile	**Lidar** • 0.5 km aerosol vertical resolution • 2 m sub-surface resolution • < 0.3% polarization misalignment • 0.0001 $km^{-1}sr^{-1}$ aerosol backscatter sensitivity at 532 nm after averaging • < 4 ns e-folding transient response • Brillouin scattering capability; Receiver FOVs: 0-60 m; 0-120 m.		
		Compare ACE observations with ground-based and model data of biological properties, land-ocean exchange in the coastal zone, physical properties (e.g., winds, SST, SSH, etc), and circulation (ML dynamics, horizontal divergence, etc)	3 4 5 6	Broad spatial coverage aerosol heights and single scatter albedo for atmospheric correction. Subsurface polarized return for typing oceanic particles	**Polarimeter** • Observation angles: 60° to 140° • Angle resolution: 5° • Degree of polarization: 1%		
		Combine ACE ocean & atmosphere observations with models to evaluate (1) air-sea exchange of particulates, dissolved materials, and gases and (2) impacts on aerosol & cloud properties	4	**Supporting Field & Laboratory Measurements** • Primary production (NPP) measurement & round-robin algorithm testing • Inherent optical properties (IOPs) instrument & protocols development, laboratory & field (coastal and open ocean) measurement comparisons • Measure key phytoplankton groups across ocean biomes (coast/open ocean) • Expanded global data sets of NPP, CDOM, DOM, pCO2, PSDs, IOPs, fluorescence, vertical organic particle fluxes, bio-available Fe concentrations		
		Assess ocean radiant heating and feedbacks	5				
		Conduct field sea-truth measurements and modeling to validate retrievals from the pelagic to near-shore environments	1 4 2 5 3 6	**Ocean Biogeochemistry-Ecosystem Modeling** • Expand model capabilities to assimilate variables such as NPP, IOPs, and phytoplankton species/functional group concentrations. • Improve model process parameterizations, e.g., particle fluxes			

* ACE focused questions are traceable to the four overarching science questions of NASA's Ocean Biology and Biogeochemistry Program [OBB1 to OBB4] as defined in the document: *Earth's Living Ocean: A Strategic Vision for the NASA Ocean Biological and Biogeochemistry Program* (under NRC review)

** See ACE Ocean Ecosystem white paper for specific vicarious calibration & validation requirements

Contents

Chapter 1

Radiometry and Phytoplankton Pigments from High Performance Liquid Chromatography

Stanford B. Hooker, NASA Goddard Space Flight Center, Greenbelt, Maryland

1.1 Introduction

A portion of the published HPLC performance metrics [*Hooker et al.*, 2005] for total Chlorophyll a (TChl *a*) and the primary pigments (PPig), which are a combination of three total chlorophylls and nine carotenoids, are included below to better explain the assessment category definitions for state of the art, quantitative, semiquantitative, and research. The latter category was named routine by the HPLC community, because "research" was thought to be too easily misunderstood as perhaps indicating the method involved was at the research stage rather than was in recurring or "routine" use for satisfying science or analytical objectives that did not require a higher level of performance. The name is not particularly important—it just needs to be agreed to. The point is to have a range of possible outcomes to accommodate the differences associated with the execution or use of any method, especially complicated ones like HPLC or radiometry, wherein there are numerous steps to properly execute before data products are produced. In this matrix, ξ is precision and ψ is accuracy; the horizontal bar represents an average and the vertical bars indicate the absolute values are averaged (*Editor's note: the typeface is different, because the source was a TeX document*).

Performance Weight, Category, and Score		*TChl* a $\bar{\xi}$	*TChl* a $\lvert\bar{\psi}\rvert$	*PPig* $\bar{\xi}$	*PPig* $\lvert\bar{\psi}\rvert$
1. Routine	0.5	8%	25%	13%	40%
2. Semiquantitative	1.5	5	15	8	25
3. Quantitative	2.5	3	10	5	15
4. State-of-the-Art	3.5	≤2	≤5	≤3	≤10
HPL (VHT) Method		*1*	*5*	*2*	*12*

For HPLC, state-of-the-art performance was conceived to be achievable only by careful attention to detail for all aspects of the complete methodology, including the filtering component in the field, or the use of next-generation hardware not available when the matrix was conceived. The quantitative category was supposed to be achievable if the protocols were strictly adhered to after a demonstrated validation phase and a regularly executed quality assurance plan. It was anticipated that this level of capability would usually be associated with calibration and validation activities (which also means a comprehensive suite of data products), and would be capable of producing an unbiased set of results that could be used as proxies for truth in an uncertainty analysis.

Semiquantitative was a transition category wherein a small number of deficiencies were not being properly resolved—perhaps because they were not important to the science objectives or were caused by method or hardware limitations that could not be overcome. Routine analysis was for practitioners working on research

Cite as: Hooker, S. B. (2022), Radiometry and Phytoplankton Pigments from High Performance Liquid Chromatography, in PACE Technical Report Series, Volume 10: ACE Ocean Product Accuracy Assessments: A record of the state of the art circa 2010 (NASA/TM – 2022-219027/ Vol. 10), edited by I. Cetinić, C. R. McClain, P. J. Werdell and M. Behrenfeld, NASA Goddard Space Flight Space Center Greenbelt, MD.

questions not tied to calibration and validation requirements, most likely focused on narrower objectives, and probably not producing a comprehensive set of data products.

These concepts need not be the ones chosen for ACE, but they sufficiently represent how many aspects of ocean color research are executed that it is hard to imagine they are not applicable. If new definitions for the categories are needed, the community needs to agree on what those definitions should be. Although this is simply stated, it was not easy to agree on the vocabulary that was chosen for HPLC. In addition, for the ACE suborbital work, the HPLC performance metric approach was used to draft and then refine the Ocean Biology Calibration and Validation Matrix (below). The emphasis with that effort was to establish each climate-quality data record (CDR) and identify the areas requiring work before we are ready for ACE, while mapping everything back to the science questions.

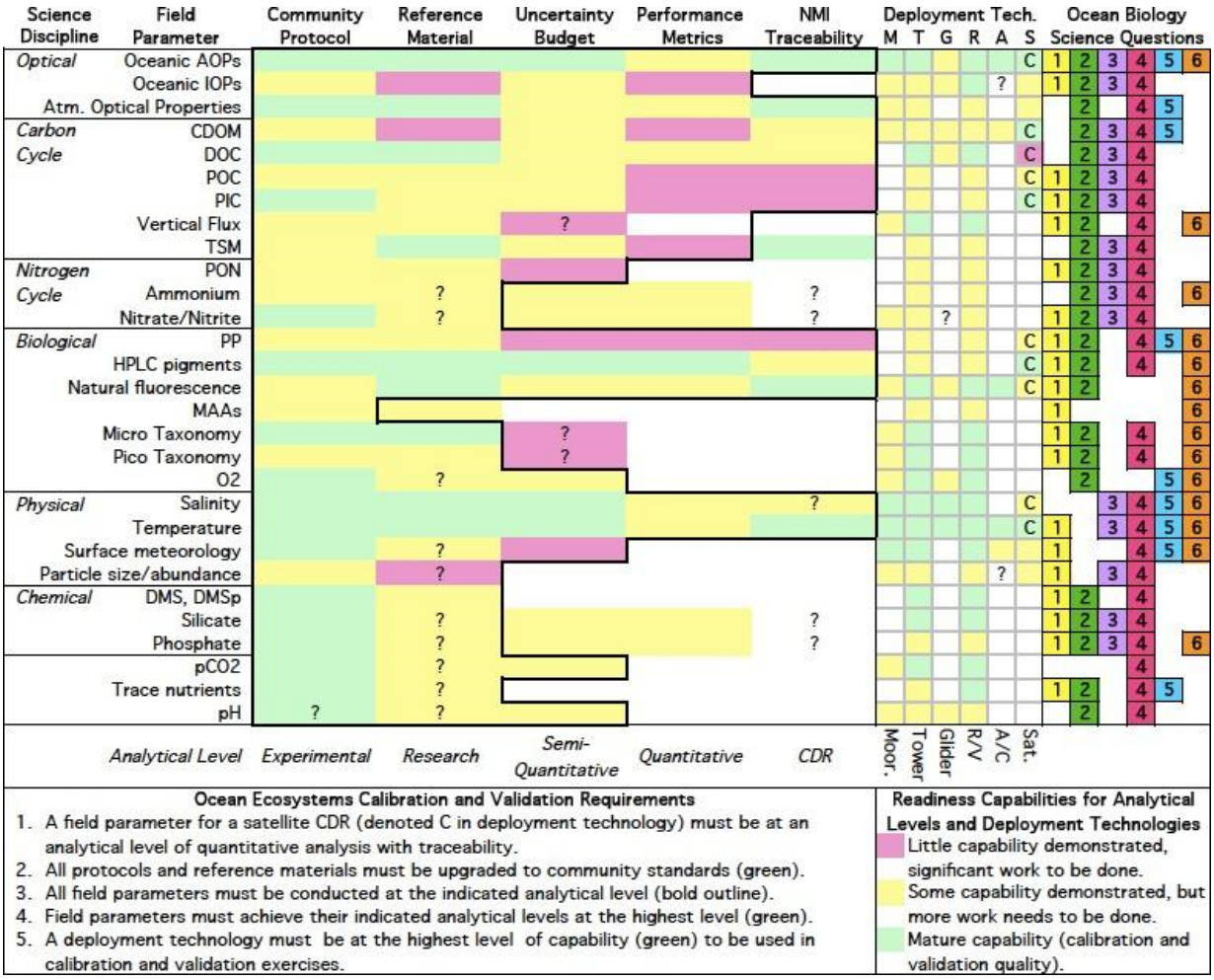

The nomenclature of the CVM with respect to the HPLC performance metrics is a little different, because the dynamic range of the full problem set is larger with many more parameters, but the intent is rather similar. The analytical levels for the parameters (along the bottom) range from Experimental to CDR, so every possible parameter can be tracked across a wide range of requirements. Category clarifications (along the top) establish what types of performance capabilities are associated with the analytical levels. For

example, a parameter at the Quantitative analytical level should have complete performance metrics, an uncertainty budget, a reference material, and a community protocol. It will not necessarily have a certified reference material (CRM), which would be traceable to a National Metrology Institute (NMI), like NIST (but it could). If a particular level is complete, the interior cell for that level is green; the other colors establish the level of incompleteness.

The bold black outline within (mostly) the interior of the matrix establishes the needed capability of a particular parameter by the time ACE launches. So, for example, Oceanic AOPs need to be at the CDR (or NMI Traceability) level, but Pico Taxonomy is only required at the Research (or Reference Material) level. For a parameter to be considered ready at the time ACE launches, all color codes should be green. The Deployment Technology and Science Questions components show how the parameters are acquired in the field and what science questions require the parameters, respectively.

The nomenclature is purposely mixed to properly harmonize common aspects for each matrix; the nomenclature is also singularly unique to emphasize specific aspects of using a matrix. In the case of the Calibration and Validation Matrix, for example, the state-of-the-art category became CDR, because producing a CDR requires our state-of- the-art capabilities and the experimental category was added to accommodate parameters that are just emerging and need to be tracked (e.g., MAAs or particle size abundance). The commonality of the language, like quantitative or semi-quantitative, provides the users of the matrices some recognizable signposts as all this information is brought together.

Performance metrics and the matrices defining them need not be static. The HPLC performance matrix is always under review and has evolved to accommodate the expanding knowledge base and comfort with how the matrix works (Hooker et al. 2010). The performance parameter matrix concept first presented for the ACE exercise is expanded here to include comments from some of the team members, who advocated the inclusion of parameters with very large uncertainties (with a maximum of 100%). In reviewing this with respect to the original CVM matrix, the presence of physical parameters for which the uncertainties are even smaller than the original quality matrix accommodated (e.g., the specifications for pressure transducers) resulted in further revisions in case all of this evolves in that direction (which is not to advocate for it to do so). The new performance parameter matrix is as follows:

Quality	**Parameter or Variable**										
Code	**Category**	**A**	**B**	**C**	**D**	**E**	**F**	**G**	**H**	**I**	**J**	**K**
T	State of the Art	1	2	3	5	7	10	13	15	20	25	30
Q	Quantitative	3	4	7	10	13	15	18	20	25	30	40
S	Semiquantitative	4	6	10	15	20	25	30	35	40	50	60
R	Research	7	10	17	25	32	40	48	55	65	80	100

There are many ways to use the scales of possible outcomes, as explained in the original message and clarified above. For the purposes of setting uncertainties from the perspective of current capabilities and how they can be applied to next-generation (ACE) planning, there are a couple of different ways for proceeding. One is to establish what can be done now, and another is to establish what is needed for ACE. For the former, the emphasis is to establish what is the present state-of-the-art category; while for the latter it is useful to make sure the current capability is set at the quantitative category of performance—but at the same uncertainty value—so there is room to improve into the state-of-the-art category. Improvements are

also achieved by moving horizontally to the left, which is towards tighter uncertainty scales. As shown below, this direction is associated with community-wide improvements, which is what next-generation thinking requires. The important point is to set "the bar" for a parameter and its anticipated outcomes (the categories), and then move the bar left–right or up–down as the process evolves.

1.2 HPLC Uncertainties

In the first message, the uncertainty for the TChl *a* concentration was set at F-T (originally E-T in the very first matrix, but the aforementioned new first column to address comments from the team means E became F). This is the performance currently being achieved for quality-assured (QA) HPLC laboratories [*Hooker et al.*, 2009], which produce the best data products and the reference values for truth in the uncertainty analyses. Although the HPLC performance metrics were designed to set this value as being in the quantitative category, for the purposes of establishing current capabilities for the ambitious science agenda for ACE, this value essentially represents the current state of the art. For future ACE work, however, the performance for TChl *a* should be set at D-Q (which has the same uncertainty), but it emphasizes the community-wide improvements that must take place (leftward shift) and it provides (upward) room to improve the current state of the art—which most assuredly must happen if the ACE science questions are going to be answered at the level they are being posed.

The concept of a QA method deserves a bit more explanation. In terms of how it is used for HPLC analysis, it is based on a) a demonstrated validation of the method, b) a strict adherence to the Protocols, and c) a continuing quantitative assessment of quality after a rigorous validation phase [*van Heukelem and Hooker*, 2011]. More recently, it also involves the quantification of all terms in the governing equation of the method [*Hooker and van Heukelem*, 2011], so a final uncertainty for all data products can be distributed with the analytical results. This rather comprehensive approach begins with the selection of the hardware [*Neeley et al.*, 2011], which is the second most critical part of controlling uncertainties (the method being the first).

During the first SeaWiFS HPLC Analysis Round-Robin Experiment (SeaHARRE-1), the original submission guidelines did not include a QA perspective [*Hooker et al.*, 2000].

The results for pigments at low concentrations were very challenging, however, and exposed the need for a QA component [*Claustre et al.*, 2004]. As the number of SeaHARRE participants increased over time and the performance metrics were developed and refined, the increase in uncertainties associated with methods not validated (NV) at the QA level was more clearly established [*Hooker et al.*, 2009].

Although there are many extreme cases of NV results with uncertainties exceeding many thousands of percent (the highest uncertainty in a SeaHARRE exercise for a NV result is 433,145% for 19'-butanoyloxyfucoxanthin), it is not useful to try and accommodate these kinds of results in a quality matrix, because it requires the matrix to be essentially unbounded. It is more sensible to make sure round robins are part of the QA assessment process and any laboratory achieving such extreme results are flagged until corrective measures have been properly implemented and a return to more reasonable uncertainties has been quantitatively verified. Although this deals properly with future results, it does not resolve what to do with the data produced before the problem was detected [*Hooker and van Heukelem*, 2009].

There are analogs to all of this in the radiometric data products for AOP measurements and the SeaWiFS Intercalibration Round-Robin Experiment (SIRREXE) activity established many of the same kinds of things for radiometry that SeaHARRE has done for HPLC. The AOP problem set is not as significantly detection limited as for many HPLC pigments, because they are primarily based on the presence of the sun, which is a very bright source, and most of the products are derived from near-surface intervals of the water column where attenuation has not acted over large spatial scales. This is not true for all parts of the spectral domain, however. For example, in the red and near infrared (NIR), the combination of high light attenuation and poor vertical sampling resolution routinely creates significant challenges and higher uncertainties.

In the progression from SIRREX-1 (1992) to SIRREX-8 (2001), the emphasis changed from methodological investigations to improve sensor calibration [*Johnson et al.*, 1999] and field stability [*Hooker and Aiken*, 1998] to overall method evaluation [*Hooker et al.*, 2002b] and verification of quality [*Johnson et al.*, 2003; *Meister et al.*, 2002]. As the emphasis changed, the types of things that were revealed or confirmed were very much associated with understanding if the method involved was validated, whether or not the Protocols were followed, and what QA procedures were applied.

Inevitably, the most significant problems that were uncovered, for example, poor immersion factors for a subset of AOP sensors [*Zibordi et al.*, 2004]were a direct consequence of one or more omissions in these three basic requirements. Ultimately, new protocols were devised [*Hooker and Zibordi*, 2005a] to strengthen any procedures found to have unnecessary weaknesses, for example, they were difficult to implement, so they were not being executed frequently enough to detect problems.

As the radiometric uncertainty budgets were being initially estimated, the focus was expanded from calibration to include differences in the data processing [*Siegel et al.*, 1995] and field acquisition techniques [*Hooker and Maritorena*, 2000] being used for the data products submitted to databases. Broader activities were pursued to confirm the initial values [*Hooker et al.*, 2002a] and to expand the emerging matrix of information. The latter included revisiting earlier activities, like data processing [*Hooker et al.*, 2001] and adding more diverse aspects of the field observation problem [*Hooker et al.*, 2004].

In some cases, multifaceted experiments were conducted in the field to focus on specific aspects of the problem set, like the importance of bidirectional corrections to AOP data products [*Hooker and Morel*, 2003]. In addition to providing more detailed uncertainty budgets, the continuing inquiries into explaining differences between investigators led to further refinements in the Protocols associated with AOP methods [*Hooker and Zibordi*, 2005b]. The culmination of all these contributions was the ability to provide a significantly complete matrix of AOP uncertainties based on a large diversity of QA principles [*Hooker et al.*, 2007]. Although the QA approach used in the HPLC and radiometric disciplines appears different based on the summaries given above, they are actually rather similar. Both activities placed a significant emphasis on validating the method being used, adhering to the Protocols, and ensuring a continuing assessment of quality. Consequently, both disciplines produced sufficient information to provide uncertainty estimates for both QA and NV methods, which are given below. The current capabilities of the QA methods are chosen as state of the art, but placed to the right in the matrix, so there will be room in the matrix for the future evolution needed for ACE (the benefits of this way of thinking are clarified below when the ACE version of all of this is presented). In addition, the matrix is now shown with colors to help correlate the two types of parameters (QA and NV) with the matrix entries.

QualityParameter or Variable											
Code	**Category**	**A**	**B**	**C**	**D**	**E**	**F**	**G**	**H**	**I**	**J**	**K**
T	State of the Art	1	2	3	5	7	10	13	15	20	25	30
Q	Quantitative	3	4	7	10	13	15	18	20	25	30	40
S	Semiquantitative	4	6	10	15	20	25	30	35	40	50	60
R	Research	7	10	17	25	32	40	48	55	65	80	100

Current HPLC Uncertainties for QA Analyses:

- TChl *a* F-T
- PPig H-T (TChl *b*, TChl *c*, Caro, Allo, But, Diato, Diad, Fuco, Hex, Peri, and Zea)
- Ancill. J-T (Phytin *a*, Phide *a*, Prasino, etc.)

Current HPLC Uncertainties for NV Analyses:

- TChl *a* F-S
- PPig H-S (TChl *b*, TChl *c*, Caro, Allo, But, Diato, Diad, Fuco, Hex, Peri, and Zea)
- Ancill. J-S (Phytin *a*, Phide *a*, Prasino, etc.)

QualityParameter or Variable											
Code	**Category**	**A**	**B**	**C**	**D**	**E**	**F**	**G**	**H**	**I**	**J**	**K**
T	State of the Art	1	2	3	5	7	10	13	15	20	25	30
Q	Quantitative	3	4	7	10	13	15	18	20	25	30	40
S	Semiquantitative	4	6	10	15	20	25	30	35	40	50	60
R	Research	7	10	17	25	32	40	48	55	65	80	100

For the next-generation (ACE) problem set, tighter uncertainty budgets are needed, but exactly how much has not been determined—that is one of the objectives of this exercise. Consequently, it seems sensible to set the new objectives based on what seems possible based on what SeaHARRE has indicated is most likely achievable. The new objectives should then be placed at the Q and S levels to ensure there is room to improve upwards towards T, if that extra performance is needed. Remember that improvements are also possible by moving to the left in the matrix, but that will require that both QA and NV improve contemporaneously. The latter is mostly associated with the maturing of an entire community, whereas the former is usually achieved by a subset of the community.

Next-Generation (ACE) HPLC Uncertainties for QA Analyses:

- TChl *a* D-Q
- PPig F-Q (TChl *b*, TChl *c*, Caro, Allo, But, Diato, Diad, Fuco, Hex, Peri, and Zea)

- Ancill. I-Q (Phytin *a*, Phide *a*, Prasino, etc.)

Next-Generation (ACE) HPLC Uncertainties for NV Analyses:

- TChl *a* D-S
- PPig F-S (TChl *b*, TChl *c*, Caro, Allo, But, Diato, Diad, Fuco, Hex, Peri, and Zea)
- Ancill. I-S (Phytin *a*, Phide *a*, Prasino, etc.)

Although HPLC is a mature technique, the uncertainties in pigments are not uniform: chlorophyll *a* (the dominant pigment in natural samples) has the lowest uncertainty, the other chlorophylls and principal carotenoids have higher uncertainties, and the degradation pigments plus the remaining carotenoids have the highest. In many of the latter cases, these uncertainties are not within the established accuracies for ocean color calibration and validation activities—particularly for future mission requirements. One reason for the elevated uncertainties is the absorption coefficient for each individual pigment is either a) unknown, so analysts choose a surrogate value, or b) has been experimentally determined, but with differing levels of quality (and none have uncertainty estimates). In both cases, analysts use a variety of different procedures to select an absorption coefficient for a pigment, but there is no consistency in the choosing—except for a small number of pigments with a narrow range of choices, like chlorophyll *a*. The absorption coefficient is a first-order variable in the calibration of an HPLC system, so the variance in choosing a value directly influences the final uncertainty in quantitating an individual pigment. Aspects of this problem are represented in the material presented here, but the full uncertainty remains unquantified and will need to be resolved for a mission like ACE. Part of the difficulty is HPLC methods use a variety of solvent systems and absorption coefficients are not available for all the solvents being used (the most common are 90% acetone, 100% acetone, 100% methanol, and 100% ethanol). The QA results presented above rely almost exclusively on the Van Heukelem and Thomas [2001] method, which uses 90% acetone as the extraction solvent. A summary of the full problem to be addressed is as follows:

1. The time period over which the laboratory experiments were performed is very large and covers 1938–1994, inclusive. The majority of the laboratory work was done in the 1960s, with diminished contributions from the 1970s and later. Almost all of this work predates the development of the methods commonly being used for marine studies.

2. Most of the pioneering work done before the 1960s has been replaced with newer results, with the notable exception of Lut (established in 1938 and only for 100% ethanol). Curiously, more recent results are not always at the highest confidence level. For example, the 1975 value for chlorophyll *b* in 90% acetone is of a lesser quality with respect to the values published from 1960–1965.

3. Very few pigments have entries as a function of the four principal solvents, and many pigments have no experimentally determined values. For those pigments with values involving two or more solvents, the change in absorption associated with a change in solvent can be significant. For example, the absorption coefficient for Diadino ranges from 223–250 across three solvents, which is approximately a 10% change.

4. Results from the modern era (defined here as after 1985, because nuclear magnetic resonance (NMR) can be used to check the purity of the pigment) are very few in number. For example, only two primary pigments, Fuco and Diato, have the highest confidence and both are for 100% acetone (none of the SeaHARRE methods use 100% acetone as a solvent).

5. None of the pigments used in the quantitation of TChl *a* have the highest confidence (although the most recent value for 100% methanol would be considered modern)—but most importantly, many of the constituent pigments have no experimentally determined values at all (e.g., DVChl *a* and Chlide *a*. Fortunately, the Chl *a* values represent the broadest inquiries of all the pigments, and within each solvent they span a rather narrow range of possible values (so reasonable agreement between analysts is assured).

In summary, many absorption coefficients being used by marine HPLC analysts today are not the most recent, or the most reliable. Although citations exist for many of the choices analysts make, the endpoint is not always a laboratory experiment based on the solvent system for the HPLC method being used. The calibration-to-quantitation applicability of the absorption coefficient with respect to an individual method—and the fact that all analysts are bound together by the value they select from the published literature—makes it perhaps the single most important term in HPLC analysis. The vexing aspect of this parameter is there is no theoretical formulation whose terms might be approximated or computed—*it must be determined experimentally, which means the quality of the empirical value is a direct byproduct of the rigor applied to the laboratory protocol.*

1.3 Radiometric Uncertainties

For the radiometric parameters, the situation is a little more simplified, because the dynamic range in the possible outcomes is a bit more constrained, but there are aspects that are more complicated because water type becomes more important and there are two different activities to keep track of: vicarious calibration and algorithm validation. And, of course, there is the QA and NV partition. Each of these aspects of the full dynamic range of the problem can be thought of as another dimension in a matrix. Although all possible dimensions will ultimately need to be represented, a smaller number are presented below to make the presentation easier to absorb. The dimensions change as the presentation unfolds, so an example for each one is available.

From a historical point of view, vicarious calibration will usually be planned and executed as an exclusively QA level of analyses in open-ocean waters, but as shown by Bailey et al. [2008], properly screened algorithm validation data sets using a “relaxed” chlorophyll criteria can be used successfully for this exercise. Rather than have two types of vicarious calibration data, it is most useful to simply have the QA level of data for this activity, because the community will always try and use the best data for vicarious calibration, but now with the understanding that the best algorithm validation data can also be used. In most cases, therefore, these data will always represent the present state of the art.

In addition, vicarious calibration data are assumed to be needed only at the wavelengths associated with the satellite sensor, so right now that means mostly channels in the visible domain; red channels are part of the band set, but they are not really used at the same level as the blue-green wavelengths in the vicarious calibration process. Next-generation satellites will extend measurements into the UV and SWIR regions. From a generalized perspective, all channels are expected to be used with equal efficacy, although their performance characteristics will not be uniform. The current mission planning discussions assume all next-generation channels will have comparable levels of uncertainty, but at this point, it is appropriate to reserve some room in the uncertainty budget for those channels that are going to be particularly challenging from a mostly open-ocean (but most likely closer to the coast) perspective. Once again, notice how the next-generation (ACE) uncertainties are set by moving the present capabilities down and to the left in the matrix.

Quality	Parameter or Variable											
Code	**Category**	**A**	**B**	**C**	**D**	**E**	**F**	**G**	**H**	**I**	**J**	**K**
T	State of the Art	1	2	3	5	7	10	13	15	20	25	30
Q	Quantitative	3	4	7	10	13	15	18	20	25	30	40
S	Semiquantitative	4	6	10	15	20	25	30	35	40	50	60
R	Research	7	10	17	25	32	40	48	55	65	80	100

Present Vicarious Calibration Radiometric Uncertainties (QA):

- Lwn C-T (Blue-Green) E-T (Red)

Next-Generation (ACE) Vicarious Calibration Radiometric Uncertainties (QA):

- Lwn B-T (UV, Blue-Green) D-T (Red, NIR, and SWIR)

Considering now algorithm validation, there is the added difficulty of water type, because data acquisition and data processing are much more challenging in turbid (frequently coastal) waters than in clear (usually open ocean) waters. For example, many instruments do not have the vertical resolution needed to resolve the optical complexity of coastal waters wherein one or more thin layers of differing water masses can be present in the water column. The most common example is fresher river water overlying saltier ocean water. Optical complexity is not exclusive to the coastal zone, however; in polar regions, melt water can significantly influence near-surface optical properties.

Data processors can contribute many sources of uncertainty, regardless of the protocols used during data acquisition. The assumption here is the heightened priority of vicarious calibration plus the desire to obtain the data in optically simpler water masses ensures data processing uncertainties are kept at the lowest level possible for that activity. For example, some practitioners collecting AOP data do not use a pressure tare to correct an absolute pressure gauge (the most common type used with in-water profilers) for the atmospheric contribution or a properly executed dark current measurement sequence to remove bias voltages for each stage of the gain amplification circuit. It is highly unlikely these types of correction would be omitted from the processing applied to a vicarious calibration data set.

Algorithm validation, by necessity, covers a much larger dynamic range in water types and science objectives, so data processing uncertainties can be significant and need to be considered. A recurring aspect of the data processing problem occurs when the focus of the science shifts and the numerical schemes have not been revised to accommodate the change. For example, the use of built-in features established for open-ocean data sets (like binning) can potentially bias the data products if data collection switches to turbid water. Similarly, assumptions about what uncertainty sources are negligible (e.g., instrument self-shading) need to be re-evaluated when there are large changes in the water masses being sampled.

Rather than explore each uncertainty associated with data processing, and given that the ACE science questions shift the emphasis from being exclusively open ocean to also including coastal waters, the minimization of data processing uncertainties are assumed to be a properly executed part of the change. This places pressure on both the data acquisition and the data processing activities, because the two

become more and more linked as the water depth decreases and the optical complexity increases. In this situation, even rather simple data products, like the diffuse attenuation coefficient (Kd)— which does not require a calibrated sensor (although, it must be stable over the time period needed to collect the data)— can be significantly affected if the technology being deployed cannot vertically resolve the optical complexity of the water column over the spatial scale of interest.

Uncertainties are also influenced by vocabulary and symbology as discussed by Hooker and Van Heukelem [2010] for HPLC analyses. Regardless of the intended use of the vocabulary and symbology, it is important to remember the formulations used to create data products require an understanding of the practices and procedures they represent. It is not enough to simply master the lexicon, particularly when dealing with literature for which the level of detail is not in keeping with the specificity needed here— some deeper investigation will probably be needed to establish whether or not the parameters involved are properly defined or represented. For radiometric parameters, the bulk Kd parameter, denoted Kb here, is significantly influenced by the presence of multiple definitions and differing numerical schemes.

The present algorithm validation uncertainties for radiometric QA analyses begins with the most commonly used variable, which is the remote sensing reflectance (Rrs). Rather than establish uncertainties as a function of wavelength, the presentation is simplified by using a typical spectral value, while emphasizing the ACE perspective of changing from the open ocean to optically complex waters. Increases in uncertainties for the latter are influenced by the absence of agreed upon bidirectional correction schemes and aliasing from inadequate vertical resolution for many instrument systems, to name two of the most obvious. Because in-water uncertainties across the present wavelength domain for ocean color remote sensing are slightly higher than above-water uncertainties, the former are used. In a full multidimensional presentation, several matrices would be needed for each parameter and that is not attempted here (as discussed earlier).

QualityParameter or Variable												
Code	**Category**	**A**	**B**	**C**	**D**	**E**	**F**	**G**	**H**	**I**	**J**	**K**
T	State of the Art	1	2	3	5	7	10	13	15	20	25	30
Q	Quantitative	3	4	7	10	13	15	18	20	25	30	40
S	Semiquantitative	4	6	10	15	20	25	30	35	40	50	60
R	Research	7	10	17	25	32	40	48	55	65	80	100

Present Algorithm Validation Radiometric Uncertainties (QA):

- Rrs(spec) D-T (open ocean); F-T (optically complex)

Simpler variables are important to ocean color research, like Kd, as are higher order variables based on Rrs, like the normalized water-leaving radiance (denoted Lwn). Again, typical uncertainties for the present ocean color perspective are assigned for open ocean and optically complex waters.

QualityParameter or Variable												
Code	**Category**	**A**	**B**	**C**	**D**	**E**	**F**	**G**	**H**	**I**	**J**	**K**

T	State of the Art	1	2	3	5	7	10	13	15	20	25	30
Q	Quantitative	3	4	7	10	13	15	18	20	25	30	40
S	Semiquantitative	4	6	10	15	20	25	30	35	40	50	60
R	Research	7	10	17	25	32	40	48	55	65	80	100

Present Algorithm Validation Radiometric Uncertainties (QA):

- Kd(490) C-T
- Kd (spec) D-T
- Lwn E-T (open ocean); G-T (optically complex)

Next-Generation (ACE) Algorithm Validation Radiometric Uncertainties (QA) are formed from the now familiar shift down and to the left of the present values:

- Rrs(spec) B-Q (open ocean); D-Q (optically complex)
- Kd(490) A-Q
- Kd (spec) B-Q
- Lwn C-Q (open ocean); E-Q (optically complex)

All of the values presented here are either thresholds of what is presently possible or targets for what needs to be possible for ACE. In either case, the two-dimensional aspect of the matrices allows the objectives associated with the thresholds to always be satisfied, at some level—it is not possible to completely fail in this approach, as long as the result is within the boundaries of the matrix. For example, if the uncertainty for Rrs is specified as C-Q (7%) and the actual value after a thorough analysis is 10%, the parameter can be classified as D-Q or C-S. The former retains the quantitative part of the original objective and the rightward shift is an adjustment in the community capability for producing the parameter; the latter retains the community capability, but adjusts the analytical level being achieved (semiquantitative replaces quantitative). Either option retains some part of the original objective. Deciding on which option should be used is simply a function of determining what problems drove the uncertainty to a higher level.

To provide distinction, each matrix is organized a little differently. As discussed above, there are also commonalities that are useful to the objective of producing a larger capability for discussing uncertainties. The mix of differences and likenesses can be confusing in the beginning, however. To ensure a proper appreciation of the intent behind what is presented here, please note the following: a) the HPLC performance matrix is organized with state-of-the-art performance as the bottom row, b) the CVM is organized with the performance categorized as columns (not rows), and c) the uncertainty matrices are organized with state-of-the-art performance as the top row.

Within the three matrices the mid-range performance categories (quantitative and semiquantitative) have the same vocabulary and are expected to be the same. The end- point categories are allowed to be different (but with some clarified commonality) to accommodate the unique objectives of each matrix.

Within the uniqueness requirement, the CVM has an added category to ensure emerging data products can be tracked properly and accommodated within mission planning exercises (like ACE).

1.4 Editorial note on Chapter 1

When this chapter was written, in 2010-2011 period, listed approaches and references were considered state of the art. Current NASA community protocols on collection of radiometric data are outlined in IOCCG series report by *Zibordi et al.* [2019].

Chapter 2

Euphotic depth

Zhongping Lee, University of Massachusetts, Boston, Massachusetts

2.1 Parameter Description

Euphotic-Zone Depth, $Z_{1\%PAR}$, was operationally defined as the depth where 1% of surface PAR (photosynthetic available radiation, 350 – 700 nm or 400 – 700 nm) *[Kirk, 1994]* remains. In a rule of thumb, $Z_{1\%PAR}$ indicates the thickness of photosynthetic-active layer (doesn't suggest no photosynthesis below this layer) of the upper ocean column. The general range of $Z_{1\%PAR}$ is:

Ocean: ~40 to 200 m

Estuaries/river plumes: ~1-50 m

2.2 Measurement Methodology Descriptions:

Because $Z_{1\%PAR}$ measures the relative amount of PAR in the water column, quantification of $Z_{1\%PAR}$ relies on the measurement of vertical profiles of PAR, or vertical profiles of spectral downwelling irradiance (Ed(λ), 350≤λ≤700 nm or 400 – 700 nm). When it is Ed(z,λ) measured, spectral integration will provide downwelling irradiance in the visible range ($E_{vis}(z)$), and a 1% depth ($Z_{1\%Evis}$) can be derived from $E_{vis}(z)$. The difference between $Z_{1\%PAR}$ and $Z_{1\%Evis}$ is under 10% [*Morel and Gentili*, 2004]. Measurement of PAR can be achieved with a commercial PAR sensor (e.g., Biospherical Instruments, Inc.). Measurement of spectral Ed can be achieved with a HyperPro (Satlantic, Inc.). There are also measurements of Ed(z,λ) with mutli-band instruments (e.g., SATPRO0027, Satlantic, Inc). To best get $Z_{1\%}$ from such measurements, multi-band Ed(z,λ) need to be interpolated to hyperspectral Ed(z,λ), then $Z_{1\%}$ can be calculated following the steps of calculating $Z_{1\%Evis}$ from hyperspectral Ed(z,λ).

2.3 Accuracy and Precision

Mathematically, $Z_{1\%PAR}$ is the depth (z) that satisfies

$$\frac{PAR(z)}{PAR(0^-)} = 0.01$$

.

Because there is no "standard" $Z_{1\%PAR}$ as a reference or for calibration, it is hard to quantify the accuracy of field measured $Z_{1\%PAR}$. In addition, because $Z_{1\%PAR}$ is a field-measured property (in contrast to lab measurements), precision of $Z_{1\%PAR}$ depends on 1) the precision of the instrument used and 2) the precision of operating the instrument in the field. On the instrument part, because the precisions of commercial PAR sensors are very high, PAR instrument itself has nearly negligible impact on the precision of $Z_{1\%PAR}$. On the operational part, the precision of $Z_{1\%PAR}$ will depend on the precision of obtaining measurements at "0 depth". The impact of this on the precision of $Z_{1\%PAR}$ could be a 0.5 – 1 meter. Depth (z) can be measured in the field with a precision higher than 0.01 m.

Cite as: Lee, Z (2022), Euphotic Depth, in PACE Technical Report Series, Volume 10: ACE Ocean Product Accuracy Assessments: A record of the state of the art circa 2010 (NASA/TM – 2022-219027/ Vol. 10), edited by I. Cetinić, C. R. McClain, P. J. Werdell and M. Behrenfeld, NASA Goddard Space Flight Space Center Greenbelt, MD

2.3.1 Quality assurance procedures

Because $Z_{1\%PAR}$ measures the relative amount of PAR(z) (or $E_{vis}(z)$) to PAR(0) (or $E_{vis}(0)$), obtain accurate measurement and determination of PAR(0) (or $E_{vis}(0)$) is very important. To achieve best $Z_{1\%PAR}$ in the field: Keep all instrument calibration (radiometric and spectral) up-to-date.

1) Operate the instruments far away from operationally ship/boat to minimize impacts from ship/boat.
2) Obtain measurements of downwelling PAR (or E_{vis}) just above the surface to ensure better measurement of PAR(0)
3) Try to obtain multiple casts if time allowed.

2.4 Standard Accuracy/Error Analysis Criterion & Statistics Description:

A recent study [*Shang et al.*, 2011] found that the difference between $Z_{1\%PAR}$ derived from PAR(z) and $Z_{1\%Evis}$ derived from $E_{vis}(z)$, all measured in the field, is ~7%. This can be considered as the upper limit of $Z_{1\%PAR}$ uncertainty from field measurements. Although many decimal points could be obtained in calculated $Z_{1\%PAR}$, one digit after the decimal point is considered significant enough (another way of measuring "precision"). In other words, if the calculated $Z_{1\%PAR}$ is 15.6432 meter, a report of 15.6 meter is precise enough to represent field measured $Z_{1\%PAR}$. In addition, for $Z_{1\%PAR}$ measurement and reporting, the following information should be included:

1. Solar zenith angle
2. Cloud information (Sun is in clouds or not during the casts)
3. Range, average, and coefficient of variation of $Z_{1\%PAR}$ if there are multiple casts.

2.5 Parameter Accuracy Assessment and Rationale:

Category	**Measurement Method**							
	A	B	C	D	E	F	G	H
State of Art **Quantitative** **Semiquantitative** **Research**	x	x	x					

Define Measurement Type

A: PAR sensor, B: Hyper-spectral Ed, C: Multi-spectral Ed

2.6 Editorial note on Chapter 2

When this chapter was written, in 2010-2011 period, listed approaches and references were considered state of the art. Current NASA community protocols on collection of radiometric data are outlined in IOCCG series report by *Zibordi et al.* [2019].

Chapter 3

Photosynthetically Available Radiation (PAR)

Robert Frouin, Scripps Institute of Oceanography, San Diego, California

3.1 Parameter Description

Photosynthetically Available Radiation (PAR) is defined as the solar quantum flux (i.e., number of solar photons per unit of time and surface) available for aquatic photosynthesis. It is expressed in units of Einstein/m^2/day (one Einstein is one mole of photons, i.e., 6.023×10^{23} photons). The spectral range of PAR contains wavelengths that intervene in the chemical reactions of photosynthesis, and was designated by the SCOR/UNESCO Working Group 15 as 350-700 nm *[Tyler, 1966]*. For practical reasons (e.g., lack of measurements in the ultraviolet), 400-700 nm is often used in the definition of PAR. Neglecting the ultraviolet part is not dramatic, because ultraviolet light contributes only 5 to 7% to the energy flux reaching the ocean surface *[Sakshaug et al., 1997].* In clear waters, ultraviolet light may penetrate deeper than green, yellow, and red light, and the percentage of ultraviolet light may reach 15% at the base of the euphotic layer. In coastal waters, neglecting ultraviolet light is inconsequential, because this light is quickly absorbed as it penetrates the surface, due to relatively high concentrations of particulate and dissolved matter. In the underwater environment, sunlight coming from all directions, i.e., scalar PAR, is relevant to photosynthesis. An important variable, however, is the amount of sunlight reaching the surface in the upper hemisphere, i.e., downward plane PAR. In the following, *PAR refers to the downward solar quantum flux reaching the horizontal plane just above the ocean surface in the spectral range 400-700 nm*, i.e.,

$$PAR = \int_{400\,nm}^{700\,nm} (\lambda/hc)\, E(\lambda)\, d\lambda$$

where λ is wavelength, E is spectral downward plane irradiance (energy per unit of time, surface, and wavelength), h is the Plank constant, and c is the velocity of light. Since the energy of a photon is hc/λ, $(\lambda/hc)E(\lambda)d\lambda$ is the number of photons (per unit of time and surface) generating radiant power $E(\lambda)d\lambda$.

The range of instantaneous PAR is 0-200 Einstein/m^2/day, with the largest values corresponding to very clear atmospheres and the sun at zenith. Daily variability, governed primarily by the sun zenith angle, may cover this range. In some situations, larger values (by up to 15%) may be encountered, due to reflection by the side of clouds. The range of daily PAR, computed as the average time integral over a day (24 hours) of instantaneous PAR, is reduced to 0-70 Einstein/m^2/day. The largest values are encountered in sub-tropical regions, generally less cloudy, around the summer solstice. Seasonal variability is regionally dependent, with the largest changes occurring at high latitudes (45 Einstein/m^2/day) and the lowest at low latitudes (15 Einstein/m^2/day). The range of annual PAR is further reduced to 10-55 Einstein/m^2/day. Inter-annual variability is usually small (i.e., a few Einstein/m^2/day), but may reach 20% in the tropical Pacific due to El Nino/Southern Oscillation.

Cite as: Lee, Z (2022), Euphotic Depth, in PACE Technical Report Series, Volume 10: ACE Ocean Product Accuracy Assessments: A record of the state of the art circa 2010 (NASA/TM – 2022-219027/ Vol. 10), edited by I. Cetinić, C. R. McClain, P. J. Werdell and M. Behrenfeld, NASA Goddard Space Flight Space Center Greenbelt, MD

3.2 Measurement Methodology Descriptions:

Instruments for the direct measurement of PAR are called quanta meters. They are designed to respond equally to quanta regardless of wavelength. Since photo-detectors do not respond equally to quanta in the photosynthetic range, the relative response in various parts of the spectrum is adjusted using colored filters [*Kirk*, 1994]. If a wide-band detector were used without adjustment, errors would be made in converting the measured flux of energy into flux of quanta that may reach a few percent depending on the spectral distribution of energy, i.e., meteorological conditions *[Morel and Smith, 1974]*.

Spectroradiometers measuring downward plane irradiance in narrow spectral bands covering the photosynthetic range give also access to PAR. In this case, PAR is obtained by integration of the irradiance measured in the individual bands after normalization by photon energy (Equation 1).

Note that the cosine collector of the instruments must be positioned horizontally for accurate PAR measurements. This may be difficult to achieve onboard ship at sea, and instruments need to be gimbaled and/or information about orientation should be recorded (e.g., to eliminate data acquired when the tilt is not negligible). The instruments should also be installed above platform structures that may mask part of the sky and reflect unwanted sunlight.

3.3 Standard Accuracy/Error Analysis Criterion & Statistics Description:

Precision of PAR measurements by commercial above-water quanta meters and spectroradiometers is generally excellent and not an issue. Accuracy is limited by the absolute calibration, traceable to NIST to within ±5%, the cosine response, which may deviate from the true cosine response by ±3% between 0 and 70 degree incidence angle, the dependence on azimuth angle, less than ±1%, the detector linearity, within ±1%, and the temperature dependence, at most ±0.2% per degree C. Regarding stability, the instrument response may exhibit ±2% change over a one year period. Therefore, depending on the instrument, solar illumination conditions, and frequency of calibration, the accuracy of PAR measurements varies typically between ±5 and 10%.

3.4 Parameter Accuracy Assessment and Rationale:

Category	**Measurement Type**							
	A	B	C	D	E	F	G	H
State of Art								
Quantitative	X	X						
Semi-quantitative								
Research								

Define Measurement Type

A: Quantum flux in photosynthetic waveband (Quanta meter); B: Spectral energy flux (Spectroradiometer)

3.5 Editorial note on Chapter 3

When this chapter was written, in 2010-2011 period, listed approaches and references were considered state of the art. Current NASA community protocols on collection of radiometric data are outlined in IOCCG series report by *Zibordi et al.* [2019].

Chapter 4

Inherent Optical Properties: absorption, scattering, and beam attenuation coefficients

Norman Nelson, University of California Santa Barbara, Santa Barbara, California

4.1 Parameter Description

Parameters: Spectral absorption, scattering, and beam attenuation coefficients, a(λ), b(λ), c(λ)

Ocean: 10^{-4} - 1 m^{-1}

Coastal/Inland waters: 0.1 - 10 m^{-1}

Inherent optical properties (IOPs) are dimensional optical quantities that are independent of the in situ radiance distribution, and are therefore a direct function of the composition and properties of the hydrosol [*Preisendorfer*, 1976]. Ocean color is directly related to inherent optical properties via a relationship that connects remote sensing reflectance to IOPs, $R_{rs}(\lambda) = f[a(\lambda) / a(\lambda)+b_b(\lambda)]$, where a and b_b are the inherent optical properties absorption and backscattering [*Gordon et al.*, 1988]. Therefore, IOPs are a key toward interpreting ocean color in terms of the biogeochemical properties of the water column. Fundamental IOPs are discussed here – other IOPs are partitioned from the fundamental measurements by various methods such as filtration, difference between products, assumption of pure water IOPs (Table 4.1 & 4.2). The fundamental IOPs are not always directly measurable and are sometimes derived from measurements of the partial coefficients by summation or inference.

IOPs are quantified as Naperian (natural logarithm) coefficients, where the parameter describes the exponential decline of light flux in a thin collimated beam through an absorbing and/or scattering medium over a discrete distance. Absorption coefficient (a) refers to decrease in flux due to absorption, while scattering coefficient (b) refers to decrease in the flux due to scattering out of the beam. The scattering coefficient can also be seen as the integral of the volume scattering function (β) over all solid angles. The beam attenuation coefficient (c) is the sum of a and b. The backscattering coefficient (b_b) refers only to light that is scattered backward through a plane normal to the incident beam.

A complete listing of IOPs and derived variables is given in Table 1, with a current assessment of (dimensional) accuracy and precision, with some possible goals for ACE field mission measurements.

4.2 Measurement Methodology Descriptions

There are two main categories of measurements: in situ instruments for measuring absorption, scattering, and attenuation (which can be lowered into the water or emplaced in flow-through seawater systems), and laboratory methods for absorption by different components (particles, CDOM) from discrete water samples.

Two kinds of in situ absorption meters currently exist. The most commonly used is the ‘shiny tube’ absorption meter [*Kirk*, 1992], in which a collimated beam is passed through a water filled tube with reflective sides, so most of the scattered light is collected by the detector. A second kind of absorption

Cite as: Nelson, N (2022), Inherent Optical Properties: absorption, scattering, and beam attenuation coefficients , in PACE Technical Report Series, Volume 10: ACE Ocean Product Accuracy Assessments: A record of the state of the art circa 2010 (NASA/TM – 2022-219027/ Vol. 10), edited by I. Cetinić, C. R. McClain, P. J. Werdell and M. Behrenfeld, NASA Goddard Space Flight Space Center Greenbelt, MD

meter uses a water-filled integrating sphere type device [*Leathers et al.*, 2000], but this device is not commonly used at present.

Also, two kinds of beam attenuation meters are commonly used [*Pegau et al.*, 2003]. The first is a 'black tube' meter, similar to the absorbing tube except that most of the scattered light is absorbed by the tube walls and is not detected. In the second kind of attenuation meter the beam passes through open water.

In situ backscattering meters have several different designs but the concept is similar: a collimated beam illuminates a volume of water, and scattered light is collected at a fixed angle. This is a measurement of the volume scattering function at that angle. The backscattering function is then estimated as a function of the scattered light at a particular angle, assuming something about the shape of the overall volume scattering function [*Maffione and Dana*, 1997; *Pegau et al.*, 2003].

Laboratory methods are primarily used to assess component absorption, particularly by particles and dissolved materials. For particles the method most commonly used is the quantitative filter technique [*Mitchell et al.*, 2000], in which particles are collected onto a glass-fiber filter (2-4L samples) and the absorbance spectra of the filters are measured in a spectrophotometer with an integrating sphere or scattered transmission accessory. Multiple scattering within the filter is corrected using an empirical method. Detrital particle absorption is estimated by depigmenting the filter using solvents or oxidants. Spectroscopy of filtered seawater (usually 0.2 micron) is used to estimate absorption by chromophoric dissolved organic matter (CDOM), using 10 cm cuvettes or 1-2m liquid waveguide cells.

4.3 Accuracy and Precision

Accuracy and precision vary between instruments, and with wavelength, and with signal level, so a comprehensive assessment of uncertainty is beyond the scope of this document. For a well-characterized in situ instrument (WETLabs ac-meter) the precision in measurement is on the order of 0.001 m^{-1}, and for backscattering sensors the precision is about a factor of ten better, taking into account instrument noise and other factors. This level of precision results in a signal to noise level in the open ocean of about 2-5 (again, depending upon wavelength and other factors), with considerably higher signal in coastal and inland waters. For the moment absolute accuracy is not determined because of a lack of reference standards.

For spectroscopically determined absorption quantities the only current reference standard is the NIST 930 filter set. This allows verification of the photometric accuracy of the photometer component of a spectrophotometer, but makes no allowance for methodological or sample preparation errors. Photometric accuracy for spectrophotometers is on the order of 0.003 (base 10 absorbance units) which translates to ~0.07 m^{-1} (for a 10cm cuvette determination of CDOM absorption coefficient) or 0.0035 m^{-1} for a 2 m liquid waveguide cell. Replication of samples can be used to assess the total precision of the method, which is usually much better than the accuracy. No generally accepted reference standards exist for in situ instruments. Calibration is usually performed against air or ultrapure water. A similar situation exists for backscattering sensors, but it is likely that reference standards can be developed from latex sphere suspensions used to calibrate particle counters.

Development of more stable IOP instrumentation for open ocean applications, and development and distribution of reference materials that can be used to calibrate in situ instrumentation, is warranted as part of the Cal/Val program for ACE/P-ACE.

4.4 Parameter Accuracy Assessment and Rationale

Category	Measurement Method							
	A	B	C	D	E	F	G	H
State of Art								
Quantitative							X	
Semiquantitative	X	X	X		X			
Research				X		X		X

Define Measurement Type:

A: In-situ shiny tube absorption meter [a(λ)] (WETLabs ac-9, ac-s)

B: In-situ black tube attenuation meter [c(λ)] (WETLabs ac-9, ac-s)

C: In-situ backscattering sensor [$b_b(\lambda)$] (HOBILabs HS-x, WETLabs BB-x)

D: In-situ integrating cavity or similar [a(λ)] (PSICAM, HOBILabs a-sphere)

E: In-situ open beam single wavelength beam transmissometer [c] (various)

F: Laboratory particle absorption (QFT) [$a_p(\lambda)$, $a_d(\lambda)$]

G: Laboratory CDOM absorption (10 cm cell, limited to coastal waters) $a_{cdom}(\lambda)$

H: Laboratory CDOM absorption (liquid waveguide cell) [$a_{cdom}(\lambda)$]

4.5 Editorial note on Chapter 4

When this chapter was written, in 2010-2011 period, listed approaches and references were considered state of the art. Current NASA community protocols on beam attenuation are outlined in IOCCG series report by *Boss et al.* [2019b], particulate absorption in report edited by *Neeley and Mannino* [2018], draft report on CDOM absorption by *Mannino et al.* [2019], and additional notes on collection of underway optical data as outlined in *Boss et al.* [2019a].

Table 4.1: Extended list of IOPs and derived products, with some estimates for range, precision, accuracy and future requirements.

	TECHNOLOGY		CURRENT RANGES				ACE MISSION REQUIREMENTS				NOTES
IOP	*Mode*	*Method*	*Wavelength (nm)*	*Range*	*Accuracy*	*Precision*	*Wavelength (nm)*	*Range*	*Accuracy*	*Precision*	
Fundamental IOPs											
$a(\lambda)$	prof/track discrete z	shiny tube integrating cavity (IC)	412-850	0.001-10 m^{-1}	0.01 m^{-1}	0.001 m^{-1}	340-865	0-1 m^{-1}			discrete λ
$c(\lambda)$	prof/ track	black tube open beam	412-850	0.001-10 m^{-1}	0.01 m^{-1}	0.001 m^{-1}	340-865	0-1 m^{-1}			discrete λ
$b(\lambda)$	prof/ track	$c(\lambda)$ - $a(\lambda)$	412-850		0.014 m^{-1}	0.005 m^{-1}	340-865	0-1 m^{-1}			
$\beta(\lambda, \varphi)$	prof/ track	detector array		0.0012 – 5 m^{-1}		1.25e-5 m^{-1} sr^{-1}	?				discrete λ
$\beta(\lambda, \varphi_i)$	prof/ track	off-axis L	400-700	0.0024 – 5 m^{-1}		1e-4 $m^{-1}sr^{-1}$	?				discrete λ, discrete φ
$a_w(\lambda)$	lab	spectrophot. photoacoust.	450-1000	0.005 – 5 m^{-1}	?	?	300-1250				Blue+UV not well defined
$b_w(\lambda)$	lab	spectrophot.	340-1000	0.0004 – 0.011 m^{-1}	?	?	300-1250				
Derived Products from the Fundamental IOPs											
$a_p(\lambda)$	prof/ track bottle	shiny tube (a-a_{gw}) QFT(-TR)	412-850 300-800			~ 0.01 m^{-1} ~ 0.025 m^{-1}	300-800				requires path amplification correction
$a_d(\lambda)$	bottle	QFT(MeOH)	300-800			~ 0.025 m^{-1}	300-800				
$a_{ph}(\lambda)$	bottle	QFT (a_p-a_d)	350-800			~ 0.05 m^{-1}	300-800				300-400 issue with MAAs?
$a_{cdom}(\lambda)$	bottle prof/ track discrete z	spec. 10cm spec. LWC shiny tube (a-a_{pw}) IC	200-800 250-730 412-850			0.03 m^{-1} 0.005 m^{-1}	250-700 250-700 400-700				
$c_p(\lambda)$	prof/ track	black tube (c-c_{gw})	412-850				?				
$\beta_p(\lambda, \varphi_i)$	prof/ track	off-axis L (β-β_{gw})	400-700			2.5E-4 $m^{-1}sr^{-1}$	?				discrete λ, discrete φ
$b_b(\lambda)$	prof/track	off-axis L	400-700			0.001 m^{-1}	340-865				derived from β
$b_{bp}(\lambda)$	prof/track	off-axis L (b_b-b_{bgw})	400-700			0.0025 m^{-1}	340-865				discrete λ

Table 4.2: Glossary for Table 1.

a(λ)	Absorption coefficient spectrum (dimensions 1/length), Naperian
c(λ)	(Beam) Attenuation coefficient spectrum (dimensions 1/length)
b(λ)	Scattering coefficient spectrum (dimensions 1/length)
β(λ,φ)	Volume scattering function (dimensions 1/length*solid angle)
p (subscript)	Partial coefficient associated with particles
d (subscript)	Partial coefficient associated with nonphytoplankton particles
g (subscript)	Partial coefficient associated with CDOM (also subscript CDOM)
w (subscript)	Partial coefficient associated with water
ph (subscript)	Partial coefficient associated with phytoplankton (also subscript φ)
b (subscript)	Partial coefficient associated with backscattering (φ = π/2 to π)
Shiny tube	Collimated beam travels down a reflective tube, detector at far end collecting most scattered and transmitted light. Reference is air, ultrapure water. Examples: WETLabs AC-*n* Requires corrections for refractive index (T and S based) and multiple scattering.
Black tube	Collimated beam travels down an absorbing wall tube, detector at far end collecting most transmitted light. Reference is air, ultrapure water. Examples: WETLabs AC-*n* Requires corrections for refractive index (T and S based)
Integrating cavity	Integrating sphere filled with absorbing medium, point-source illumination. Reference is air or ultrapure water. Example: PSICAM
prof/track	Instruments that are suitable for profiling and/or alongtrack measurements (high temporal resolution)
discrete z	Instrument can measure profiles with limited depth resolution (a number of discrete depths)
lab	Measurement is a laboratory-only (not field) procedure
bottle	Measurements are made on discrete samples from Niskin bottle samples
detector φ array	Water volume illuminated by a collimated beam, scattered radiance is collected by an array of detectors at various angles. Example: WETLabs ECOvsf
off-axis L	Water volume illuminated by a collimated beam, scattered radiance is collected by detector at a fixed angle. Example: HOBILabs Hydroscat-6 Requires assumption of VSF shape to convert from scattering at one fixed angle to backscattering coefficient.
spectrophot.	UV-Visible or visible absorption spectroscopy. Reference is ultrapure water
LWC	Liquid Waveguide Cuvette – long path absorption cell (for nonscattering solutions such as filtered seawater for CDOM). Reference is ultrapure water. Example: WPI UltraPath Requires correction for refractive index (S based)

photoacoust.	Photoacoustic spectroscopy
QFT	Quantitative Filter Technique – measuring absorbance of particles collected on filters using UV-Vis absorption spectroscopy, corrected for multiple scattering (β-correction). Blank/reference is unloaded filter.
QFT-TR	Quantitative Filter Technique with Transmittance/Reflectance – as QFT with additional reflectance measurements (requires integrating sphere, β-correction.
QFT (MeOH)	Estimation of nonphytoplankton absorption by QFT of solvent (usually methanol)-extracted filters (Kishino method)

Chapter 5

Inherent Optical Properties: beam attenuation

Toby Westberry, Oregon State University, Corvallis, Oregon

5.1 Parameter Description

Parameters: Spectral beam attenuation coefficients, c(λ)

Ocean: 0.03 – 1 m^{-1}

Coastal/Inland waters: 1 - 10 m^{-1}

Beam attenuation (c) is a measure of the transmittance of a collimated light source through a finite pathlength and is equivalent to the sum of the absorption (a) and scattering (b) coefficients measured across the same pathlength. Specifically, the beam attenuation coefficient can be calculated by solving the Beer-Bouger-Lambert relationship such that:

$$c = \ln(TR)/r \qquad [m^{-1}]$$

where TR is the ratio of light flux measured at a detector through a sample (seawater) of pathlength, *r* [meters] to that of the light flux measured through a reference medium (pure water). Beam attenuation is a spectrally dependent measurement and contains contributions from pure water absorption and scattering, particulate absorption and scattering, and dissolved material absorption. Historically, measurements of c at ~660 nm have been widespread because dissolved material absorption is negligible in this part of the spectrum and pure water properties are known, such that the remainder is the particulate beam attenuation coefficient, $c_p(\lambda)$. The particulate beam attenuation coefficient depends on the composition of the particle assemblage; their size, shape, and internal index of refraction. For most of the ocean, $c_p(\lambda)$ is dominated by particulate scattering, but in high biomass environments absorption can be significant. Estimates of $c_p(\lambda)$ have been used as a proxy for POC, total particle volume, phytoplankton abundance, and phytoplankton growth rate.

5.2 Measurement Methodology Descriptions:

The primary tool used to measure beam attenuation is a transmissometer (sometimes called a beam attenuation meter). Commercially available transmissometers have been available for decades, though hyperspectral instruments are relatively new. There are various designs for transmissometers, but one important distinction is whether a user employs them with an open pathlength or using a flow tube which requires seawater to be actively pumped through the instrument. The two methods may not yield the same measurement due to shearing of particle aggregates, and this is an unresolved issue. In either case, transmissometers can be mounted on traditional CTD-type rosette systems, specialized optics cages, moorings, floats, gliders, or used in a flow-through manner, but considerations for each different type of deployment must be made. In the field, care must be taken to clean the source and detector windows before each use with a mild detergent solution and soft cloth and rinsed thoroughly with distilled water. Dark measurements must also be made before use to account for internal instrument noise (dark measurement) and accompanying measurements of ultra-clean MiliQ water (or similar) used as a reference. Sometimes, very deep ocean water assumed to be devoid of particles (effectively filtered

Cite as: Westberry, T. (2022), Inherent Optical Properties: beam attenuation, in PACE Technical Report Series, Volume 10: ACE Ocean Product Accuracy Assessments: A record of the state of the art circa 2010 (NASA/TM – 2022-219027/ Vol. 10), edited by I. Cetinić, C. R. McClain, P. J. Werdell and M. Behrenfeld, NASA Goddard Space Flight Space Center Greenbelt, MD

seawater) is also used as a reference measurement. A thorough review of these instruments and their use is available in Pegau et al. [2003]. One important consideration is that the measurement is only valid in a single scattering regime, which means that in clear water the pathlength can be longer and in turbid waters the pathlength must be shorter. The rule of thumb for satisfying the single-scattering criterion is to keep the optical thickness (the product of beam attenuation coefficient and pathlength) below 0.1 (strict criterion) or below 0.3 (less conservative but still acceptable criterion). Also, transmissometers, by design, have a finite acceptance angle, and hence do not measure the theoretical beam attenuation. Indeed, comparison of commercial beam-transmissometers reveal the potential for large (>40%) differences in the measured beam-attenuation which can be explained due to their difference in acceptance angle. Hence, any measurement of beam attenuation reported should also specify the acceptance angle of the instrument used.

5.3 Accuracy and Precision:

Accuracy and precision vary between instruments, and with wavelength, and with signal level, so a comprehensive assessment of uncertainty is beyond the scope of this document. For a well-characterized *in situ* instrument (WETLabs ac-meter) the precision in measurement is on the order of 0.001 m^{-1}. This level of precision results in a signal to noise level in the open ocean of about 2-5 (again, depending upon wavelength and other factors), with considerably higher signal (and uncertainty) in coastal and inland waters. For the moment, absolute accuracy is not determined because of a lack of consistent reference standards. Replication of samples can be used to assess the total precision of the method, which is usually much better than the accuracy. Calibration is usually performed against air or ultrapure water. Development of more stable IOP instrumentation for open ocean applications, and development and distribution of reference materials that can be used to calibrate in situ instrumentation, is warranted as part of the Cal/Val program for ACE/P-ACE.

5.4 Parameter Accuracy Assessment and Rationale:

Category	**Measurement Method**							
	A	B	C	D	E	F	G	H
State of Art								
Quantitative	X							
Semiquantitative								
Research								

Define Measurement Type:

A: In-situ beam attenuation [c]

5.5 Editorial note on Chapter 5

When this chapter was written, in 2010-2011 period, named approaches and references were considered state of the art. Current NASA community protocols on beam attenuation are outlined in IOCCG series

report by *Boss et al.* [2019b], and additional notes on collection of underway optical data is outline in *Boss et al.* [2019a].

Chapter 6

Inherent Optical Properties: backscattering

Emmanuel Boss, University of Maine, Orono, Maine

6.1 Parameter Description

Parameter: Backscattering coefficient, $b_b(\lambda)$

Ocean: 0.0003 – 0.01 m^{-1}

Coastal/Inland waters: 0.01 – 0.1 m^{-1}

The backscattering coefficient (b_b) is a measure of the amount of light that is lost from a collimated beam towards the backward hemisphere due to the process of elastic scattering. Specifically, b_b is calculated from measurements of light that is backscattered from one or more angles in the backward hemisphere.

The backscattering coefficient is primarily dependent upon particle concentration and to a lesser degree, on their size, shape, internal structure and effective index of refraction. Estimates of $b_b(\lambda)$ have been used as a proxy for suspended mass [SPM, *Boss et al.*, 2009], particulate organic carbon [POC, *Stramski et al.*, 2008], and phytoplankton carbon biomass [*Behrenfeld et al.*, 2005].

Uncertainty exists in the literature regarding the relative contribution of particles smaller than 0.2μm in size to the backscattering coefficient (typically particle size is expressed in terms of equivalent spherical diameter). See Stramski et al. [2004] for a thorough review of backscattering in the ocean.

6.2 Measurement Methodology Descriptions:

In this section we focus on measurements using commercially available instrumentation, though it should be noted that more unique experimental devices exist [e.g. *Chami et al.*, 2006; *Sullivan and Twardowski*, 2009]. A detailed review of the method is provided in Boss et al. [2004]. Single angle backscattering meters (e.g. HobiLabs Hydroscat, WETLabs Eco-bb), measure angular scattering (the volume scattering function, β) for a given wavelength (λ_0): centered around one angle in the backward direction (θ_0):

$$<\beta(\lambda_0,\theta_0)>=\int_{\Omega_0-\Delta\Omega}^{\Omega_0+\Delta\Omega_1}\int_{\lambda_0-\Delta\lambda_1}^{\lambda_0+\Delta\lambda_1}W_1(\Omega)W_2(\lambda)\beta(\Omega)d\lambda d\Omega \approx 2\pi\int_{\theta_0-\Delta\theta}^{\theta_0+\Delta\theta_1}\int_{\lambda_0-\Delta\lambda_1}^{\lambda_0+\Delta\lambda_1}W_1(\theta)W_2(\lambda)\beta(\theta)d\lambda\sin\theta d\theta$$

Where $W_{1,2}$ denote weighting functions for the measurement angle and wavelength respectively, and where azimuthal symmetry is assumed. Conversion to backscattering (units of m^{-1}) is based on theory and observations:

$$b_b(\lambda_0,\theta_0)=2\pi\chi(\theta_0)<\beta(\lambda_0,\theta_0)>$$

Cite as: Boss, E (2022), Inherent Optical Properties: backscattering, in PACE Technical Report Series, Volume 10: ACE Ocean Product Accuracy Assessments: A record of the state of the art circa 2010 (NASA/TM – 2022-219027/ Vol. 10), edited by I. Cetinić, C. R. McClain, P. J. Werdell and M. Behrenfeld, NASA Goddard Space Flight Space Center Greenbelt, MD

WETLabs also provides a three-angle backscattering sensor (ECO-VSF). For such a sensor the VSF is computed by fitting a 3rd order polynomial to $<\beta(\lambda_0,\theta_0)>\sin\theta_0$ using the fact that $<\beta(\lambda_0,\pi)>\sin\pi=0$ at the retroscattering angle (π).

Backscattering by water and salts needs to be taken into account as, calibration dependent, water backscattering is not taken into account when applying the manufacturer calibration constants and given that the above conversion parameter is different for sea water and particles (except near 117º, Boss and Pegau, 2001). For backscattering by water and salts see Zhang et al., 2009 .

Another method to obtain the backscattering coefficient is using in-situ or bench-top (e.g. Wyatt Technology Corp.) angular scattering meters. The backscattering coefficient is computed from the integral of the VSF (β) over the backward hemisphere (Ω_b) or assuming azimuthal symmetry (e.g. if particles are randomly oriented) integrating over scattering angle measured relative to the direction of the beam (θ):

$$b_b(\lambda)=\int_0^{2\pi}\beta(\lambda,\Omega)d\Omega\approx 2\pi\int_{\pi/2}^{\pi}\beta(\lambda,\theta)\sin\theta d\theta \quad .$$

Unfortunately today there are no ”off the shelf” instruments that can provide a high angular resolution VSF in situ.

Given that light is attenuated along the path from source to receiver, a correction for this attenuation needs to be applied [e.g. *Boss et al.*, 2004]. Unfortunately, this correction itself is VSF dependent.

6.3 Deployment

Backscattering sensor can be deployed on CTD-type rosette systems, moorings, flow through systems and specialized optics cages. It is imperative to obtain accurate values of the dark current near the time of deployment as some commercial sensors exhibit system dependent dark values, presumably due to electronic interference (resulting in very different values than those reported by the manufacturer). Some sensors also suffer from grounding problems (exhibited as noisy data) a problem that is solved if the source power is well grounded (‘clean’). These problems become particularly important to address in clear ocean water.

6.4 Accuracy and Precision:

A comprehensive assessment of uncertainty is beyond the scope of this document. For a well-characterized recently calibrated in situ instrument (WETLabs or HobiLabs) the precision in measurement is on the order of 0.00001 m^{-1} and published uncertainties for the backscattering coefficient are O(0.0001 m^{-1}) [e.g., *Dall'Olmo et al.*, 2009; *Twardowski et al.*, 2007]. The uncertainty relative to the ‘true’ backscattering coefficient can be quite large due to: (1) variability in reported conversion coefficient of O(10%), (2) uncertainties associated with the attenuation correction, and (3) uncertainties associated with the dark current.

Co-deployment of sensors built and calibrated by different manufacturers can be used to assess the total uncertainty of the method, which is usually much larger than the reported accuracy (Boss et al., 2004). Calibration is usually performed using precision optical calibration beads or using a plate of known spectral reflectance. When using beads, calibration uncertainties can be assessed and tested using another

bead of different property [e.g., *Slade and Boss*, 2006]. Commercial sensors do drift and hence, it is imperative to periodically calibrate the sensor.

6.5 Parameter Accuracy Assessment and Rationale:

Category	**Measurement Method**							
	A	B	C	D	E	F	G	H
State of Art								
Quantitative	X							
Semiquantitative								
Research								

Define Measurement Type:

A: Backscattering coefficient [b_b]

6.6 Editorial note on Chapter 6

When this chapter was written, in 2010-2011 period, named approaches and references were considered state of the art. Current NASA community protocols on collection and processing of the ship -based underway flow-through optical data are outlined in *Boss et al.* [2019a].

Chapter 7

Fluorescence Line Height and Fluorescence Quantum Yield

Michael Behrenfeld, Oregon State University, Corvallis, Oregon

7.1 Parameter Description

Oxygenic photosynthesis in phytoplankton involves light harvesting and electron transport between two pigmented reaction centers: photosystem II (PSII), which is solely responsible for oxygen evolution, and photosystem I (PSI). Both photosystems contribute to cellular chlorophyll concentration and light absorption, but in vivo fluorescence emanates almost exclusively from PSII. This chlorophyll fluorescence represents only a minor de-excitation pathway for sunlight energy absorbed by phytoplankton, but it creates a distinct peak in the color spectrum of the ocean that is readily resolved in field radiance data. A common parameter used to quantify the chlorophyll fluorescence signal is the Fluorescence Line Height (FLH) [*Gower*, 1980; *Letelier and Abbott*, 1996]. FLH represents the difference between upwelling radiance in the chlorophyll fluorescence band (typically measured at 683 nm) and the upwelling radiance that would result in the absence of fluorescence. FLH can be analytically related to the total fluoresced radiance after accounting for a number of physical and physiological effects.

The fluorescence quantum yield (FQY) is defined as the ratio of total fluoresced radiance to absorbed light energy by phytoplankton and is a measure of the efficiency with which light absorbed by phytoplankton pigments is lost as fluorescence. FQY provides information on physiological processes influencing light use efficiencies in phytoplankton, in particular non-photochemical quenching and iron limitation. There is no 'general' relationship between FQY and nutrient stress or growth rate, aside from the unique impacts of iron limitation. However, evidence does exist that FQY can increase during transient periods on non-steady-state growth.

Units of FLH are those of a spectral radiance, e.g. mW cm^{-2} um^{-1} sr^{-1} and values in the ocean calculated using the MODIS wavebands are 0-0.03 mW cm^{-2} um^{-1} sr^{-1}. FQY is dimensionless (or sometimes reported as photons fluoresced per photos absorbed) and ranges from 0 to ~0.06 in the surface ocean.

7.2 Measurement Methodology Descriptions

FLH is derived from measured upwelling radiance spectra just below the sea surface, $L_u(\lambda, 0^-)$ (above surface measurements can also be used). Measurement methodology should be the same for general AOP measurements (see related product assessment by Stan Hooker). Spectral bands used for the calculation of FLH may vary depending on the spectro-radiometer used, but three bands are required; one representing the upwelling radiance near the peak of chlorophyll fluorescence emission (e.g., 683 nm), and one band on each side of the fluorescence emission spectrum (e.g., 650 nm and 720 nm). For example, MODIS-Aqua uses 10 nm wavebands centered on 678 nm, 667 nm and 748 nm, for the peak and baseline wavebands, respectively. Assessment of the fluoresced component of the 683 nm signal is accomplished by subtracting the baseline radiance estimated through linear interpolation of the two wavelengths bracketing the chlorophyll fluorescence signal.

The fluorescence quantum yield can be derived from FLH measurements by accounting for (1) the spectral distribution of the fluorescence emission relative to the peak FLH wavelength measured

Cite as: Behrenfeld, M (2022), Fluorescence Line Height and Fluorescence Quantum Yield, in PACE Technical Report Series, Volume 10: ACE Ocean Product Accuracy Assessments: A record of the state of the art circa 2010 (NASA/TM – 2022-219027/ Vol. 10), edited by I. Cetinić, C. R. McClain, P. J. Werdell and M. Behrenfeld, NASA Goddard Space Flight Space Center Greenbelt, MD

(typically modeled as a Gaussian distribution), (2) the isotropic distribution of fluoresced light from phytoplankton, (3) internal absorption of fluorescence within phytoplankton cells, (4) spectral intensity of scalar irradiance, and (5) the spectral absorption properties of the phytoplankton community. Details can be found in Kiefer et al. [1989]. Several of these aspects can be modeled as a function of chlorophyll concentration (or diffuse attenuation at 490 nm, K_d490, e.g., Huot et al., 2005), but supporting measurements of incident spectral irradiance, $E_d(\lambda,0^+)$, and phytoplankton absorption, $a_{ph}(\lambda)$, are recommended following typical IOP and AOP protocols (Mueller et al., 2002; or see associated parameter assessments by Norm Nelson and Stan Hooker).

7.3 Standard Accuracy/Error Analysis Criterion & Statistics Description

There are no standard materials for assessing fluorescence light heights or fluorescence quantum efficiencies. See accompanying Parameter Assessments by Norman Nelson and Stanford Hooker for accuracy assessments for IOPs and AOPs.

7.4 Parameter Accuracy Assessment and Rationale

Accuracy and precision of FLH measurements should be similar to that for upwelling radiance. Error estimation for FQY calculations is difficult because of the many pieces of information required and the transformations required of them. Culver and Perry (1997) calculated FQY based on upwelling irradiance (rather than radiance), but much of the formulation is the same. The authors found that errors in fluorescence yield estimates ranged from 5.7% to 27.6%. This includes a 12% error in near-surface downwelling irradiance, 4-10% (mean equal 5%) error in downwelling attenuation coefficients. Also, replicate measurements of the angular distribution of upwelling irradiance (D_u) varied by 1.1-15.2%, with a mean error of 5.5% and uncertainties in measured phytoplankton absorption coefficients were estimated at 10.0% to 13.5%, with a mean of 10.7%.

Category	**Parameter Classification**							
	A	B	C	D	E	F	G	H
State of Art	X							
Quantitative		X						
Semiquantitative								
Research								

A: Fluorescence Line Height

B: Fluorescence Quantum Yield

7.5 Editorial note on Chapter 7

When this chapter was written, in 2010-2011 period, listed approaches and references were considered state of the art. An updated protocol was not available at the time of publication of this TM. Please check the IOCGG protocol document list at https://ioccg.org/what-we-do/ioccg-publications/ocean-optics-protocols-satellite-ocean-colour-sensor-validation/ regularly.

Chapter 8

Dissolved Organic Carbon

Antonio Mannino, NASA Goddard Space Flight Center, Greenbelt, Maryland

8.1 Parameter Description

Ocean: 34 to 120 µmol C L^{-1}

Estuaries/river plumes: 100-1000 µmol C L^{-1}

8.2 Measurement Methodology Descriptions

There are three methods for quantifying DOC that involve the oxidation of DOC to CO2 with quantitation of CO2 by infrared detection: (1) high-temperature combustion oxidation (HTCO), (2) wet-chemical oxidation (persulfate oxidation) and (3) ultraviolet oxidation. The HTCO is most common and accepted method for brackish to oceanic waters. Persulfate oxidation is not recommended for saline waters because of the interference by chloride ions in seawater with the oxidation of DOC. The persulfate oxidation method is advantageous because a much larger sample volume can be oxidized than for the HTCO method resulting in significantly higher measurement sensitivity.

There is no national or international standard for seawater DOC. However, the scientific community has accepted the deep seawater Consensus Reference Material (CRM) distributed by the Hansell Laboratory, Rosenstiel School of Marine and Atmospheric Science (RSMAS), University of Miami. The seawater CRM is analyzed at several laboratories that provide consistently high quality results to reach a consensus DOC concentration. The CRM is distributed to research laboratories in sealed ampoules at a cost of $100 per box (144 ampoules) plus shipping charges. Low carbon reference water is also available and shipped with the seawater CRM at a cost of $50 per box. Laboratories with high-grade ultra-pure water systems equipped with ultraviolet lamps can produce low carbon water of equivalent or better quality.

For detailed discussions on sample collection, preservation, and storage, see the following references: JGOFS Report No. 19 (1994), *Norrman* [1993], *Sharp et al.* [1993]; *Tupas et al.* [1994], *Sharp et al.* [1995].

8.2.1 Case 1

Collect seawater samples in duplicate or triplicate directly from Niskin bottles into pre-combusted (450 ºC for 6 hours minimum) glass sample bottles without filtration. To minimize contamination do not overflow sample bottles while filling. Wearing powder-free gloves is recommended but avoid contact with sample or any surface that will come in contact with sample. To avoid contamination during sample transfer, collect the total organic carbon (TOC) samples directly into autosampler vials. Fill vials to below the shoulder-level of the vials to prevent cracking of glass during freezing. Rinsing of sample containers with sample water may reduce artifacts due to DOC sorption to active sites on container surface. Samples should be stored frozen (-20ºC) or can be preserved with 0.1% Hydrochloric Acid (ACS plus grade or better) and stored under refrigeration (4ºC) or frozen. Filtration is necessary where particle loads yield significant quantities of particulate organic carbon (POC) - >2 µmol C L^{-1}.

Cite as: Mannino, A. (2022), Dissolved Organic Carbon, in PACE Technical Report Series, Volume 10: ACE Ocean Product Accuracy Assessments: A record of the state of the art circa 2010 (NASA/TM – 2022-219027/ Vol. 10), edited by I. Cetinić, C. R. McClain, P. J. Werdell and M. Behrenfeld, NASA Goddard Space Flight Space Center Greenbelt, MD

8.2.2 Case 2

Samples must be filtered to remove particles. Filtration can be accomplished with in-line filters at the Niskin bottle or under a gentle vacuum (<5 in Hg; oil-free vacuum pump) in a clean laboratory setting. Filter samples directly into pre-combusted glass sample containers. Collect 2 or more replicate sample vials for each discrete sample. Positive pressure filtration (10 psi) using a thoroughly cleaned stainless steel pressure vessel with ultra high purity N_2 gas (99.999% minimum) has also been used to collect DOC samples. Glass filtration equipment is recommended because it can be combusted to minimize contamination. Wearing powder-free gloves is recommended but avoid contact with sample or any surface that will come in contact with the sample. To minimize contamination do not overflow sample bottles while filling. Rinsing of sample containers with sample water may reduce artifacts due to DOC sorption to active sites on container surface. Plastic bottles (Teflon, polycarbonate, polypropylene or high-density polyethylene) may be used, though not recommended, for samples collected in coastal waters where DOC exceeds 150 µmol C L^{-1} as long as the bottles and caps (Teflon-lined or polypropylene) are cleaned with a basic detergent and acid, rinsed thoroughly with ultra-pure water, and oven-dried. There are several options for filters depending on the anticipated particle load: GF/F glass fiber filters (nominal <0.7 µm; pre-combusted in furnace at 450 ºC for 6 hours), 0.2 µm polycarbonate filters (e.g., Whatman Nuclepore, Osmonics Poretics, and Millipore Isopore), and 0.2 µm polyethersulfone filters (e.g., Pall Gelman Supor 200). The GF/F glass fiber filters are recommended because they can be rendered carbon-free by combustion in a muffle furnace. All non-combusted filters such as the polycarbonate (PC) and polyethersulfone (PES) filters can be cleaned (soaked in 10% hydrochloric acid and ultra-pure water) and rinsed with sample (50 to 100 mL) prior to use to reduce contamination. Evaluation of contamination from filtration process (including filters) is strongly encouraged. Samples should be stored frozen (-20ºC) or can be preserved with 0.1% hydrochloric acid and stored under refrigeration (4ºC) or frozen. Filtered samples may be stored on ice for short periods (<12 hours) if a freezer is not available, but acidification is recommended to minimize alteration of DOC from biological processes.

8.2.3 Quality assurance procedures

Use ultra-pure (Type I; resistivity ≥18.2 MΩ cm) and ultraviolet oxidized water (e.g., Milli-Q Gradient, Nanopure Diamond UV, etc.) with total organic carbon ≤10 µg C L^{-1} for preparation of all solutions (acids, calibration standards), filling all containers used within the instrument, and final rinsing of cleaned glassware and other materials. Water purification systems require diligent system maintenance to ensure high quality laboratory water with low DOC. A well-maintained water system can yield carbon peak area responses equivalent to that of instrument blanks. Several manufacturers equip ultra-pure water systems with TOC monitors that provide an indication of the carbon content of the water.

8.3 Standard Accuracy/Error Analysis Criterion & Statistics Description:

Absolute uncertainties for DOC cannot be determined when quantifying a complex mixture of compounds because of differences in catalytic combustion oxidative responses of carbon calibration standards (potassium hydrogen phthalate or glucose) compared to natural seawater samples. Diligent analysis of the CRM provides a way to constrain the relative uncertainty of DOC measurements. However, the CRM is not necessarily representative of the chemical composition of DOC found in coastal regions, where terrestrial organic matter may contribute significant amounts of carbon to DOC, or within a phytoplankton bloom where higher protein and lipid content may be present.

The following information should be reported: (1) DOC concentration of each sample with an estimated relative uncertainty, (2) average DOC concentration and standard deviation of the CRM, (3) average and standard deviation of DOC concentration for ultra-pure water blanks (includes instrument blank) and (4) range and average percent coefficient of variation (%CV) of replicate samples analyzed.

8.4 Parameter Accuracy Assessment and Rationale:

Category	Measurement Type							
	A	B	C	D	E	F	G	H
State of Art		3						
Quantitative		7						
Semiquantitative		10						
Research		17						

B: Dissolved Organic Carbon (DOC)

A community intercalibration on DOC analysis conducted a decade ago provides an assessment of DOC measurement accuracies that are achievable by a wide array of laboratories and instruments [*Sharp et al.*, 2002]. The results for all 53 HTCO instruments that passed the pre-screening criteria (DOC values within ±2 standard deviations of the mean) demonstrated an average %CV of 10.0% (range of 4.75 to 17.31%) for 10 natural water samples with a wide range of DOC (36 to 210 µmol C L^{-1}) and salinity (0 to seawater). The ten best Shimadzu TOC-5000 instruments yielded a %CV of 6.0% (range of 3.80 to 9.11%). Sharp et al. [2002] demonstrated that preliminary use of the DOC CRM yielded DOC reproducibility on the order of 2-6%. Several laboratories have reported agreement for DOC values to within 2% through the use of the DOC reference materials [*Hansell and Carlson*, 1998; 2001; *Hansell and Peltzer*, 1998].

8.5 Editorial note on Chapter 8

When this chapter was written, in 2010-2011 period, listed approaches and references were considered state of the art. An updated protocol was not available at the time of publication of this TM. Please check the IOCGG protocol document list at https://ioccg.org/what-we-do/ioccg-publications/ocean-optics-protocols-satellite-ocean-colour-sensor-validation/ regularly.

Chapter 9

Particulate Organic Carbon

Dariusz Stramski, Scripps Institute of Oceanography, San Diego, California

9.1 Parameter Description

Particulate Organic Carbon (POC) concentration is defined as a mass of organic carbon associated with aquatic suspended particles per unit volume of water. The most common operational definition of POC represents particulate organic carbon retained on a glass-fiber filter (Whatman GF/F). This operational definition implies that an unknown fraction of particulate organic carbon associated with many submicron particles (smaller than about 0.7 μm) is not included in the POC measurement. Note that the GF/F filter has no well-defined pore size although sometimes 0.7 μm is given as an "average" or "effective" pore size. In practicality, the GF/F filters are known to retain quite efficiently most particles larger than 0.4 - 0.5 μm.

The units of POC are mg m^{-3}. The range in the surface ocean is from about 10 to more than 1000 mg m^{-3}.

9.2 Measurement Methodology Descriptions:

The method for determining POC in seawater described here is generally consistent with JGOFS protocols [*Kadar et al.*, 1993; *Knap et al.*, 1996]. This method consists of two major steps: first, the collection of particulate matter on GF/F filters, and second, analysis of samples in a laboratory with a CHN analyzer. A CHN analyzer is a scientific instrument which can determine the elemental composition of a sample through a combustion process that breaks down substances into simple compounds which are then measured. The name derives from the three primary elements measured by the device: carbon (C), hydrogen (H), and nitrogen (N). By separating out inorganic carbon using a solvent before the analysis, organic carbon in a sample can be measured using this device.

Alternative methods not addressed in this report include in-situ filtration pumps and high-temperature combustion (HTC), where POC is estimated from the analysis of water samples as the difference between total organic carbon (TOC) and dissolved organic carbon (DOC) [*Gardner et al.*, 2003].

9.2.1 Sample acquisition

Seawater samples are typically collected from Niskin bottles triggered at selected depths during the CTD/rosette cast. Because large particles in the Niskin bottle tend to settle over time, it is desirable to gently agitate the contents of Niskin bottle before taking a sample through the spigot into the clean sample container (usually opaque polypropylene plastic bottles or carboys). This action of agitation of Niskin bottle may not, however, be easily practicable. An alternative is to sample the full volume of water from the Niskin bottle, including the volume below the spigot. This would generally ensure that all particles are collected. It is important to realize that both the samples obtained through the spigot and the entire Niskin volume may have advantages and disadvantages depending on the science objectives. Whereas the sampling of the entire volume appears to be generally most desirable because it best ensures to represent all particles including large fast-settling particles, avoiding these large particles may be advantageous in some studies such as those seeking the relationships between the inherent optical properties (IOPs) of seawater and POC. This is because the IOPs should, by definition, be measured on

Cite as: Stramski, D (2022), Particulate Organic Carbon, in PACE Technical Report Series, Volume 10: ACE Ocean Product Accuracy Assessments: A record of the state of the art circa 2010 (NASA/TM – 2022-219027/ Vol. 10), edited by I. Cetinić, C. R. McClain, P. J. Werdell and M. Behrenfeld, NASA Goddard Space Flight Space Center Greenbelt, MD

small volume of seawater (i.e., over short pathlength), so typically they do not account appropriately for the presence of relatively rare large particles.

9.2.2 Filtration

Immediately after collection, water samples are filtered on precombusted (450°C, duration of combustion typically varies between 30 min and 5 hours depending on laboratory) 25-mm Whatman GF/F filters under low vacuum (pressure differential across the filters < 0.25 atm). Filtered volumes are adjusted according to expected POC concentration. The volume can vary from a fraction of a liter in waters rich in particulate matter up to about 8-9 L in clearest oligotrophic oceanic waters [*Gardner et al.*, 2003; *Stramski et al.*, 2008]. The selection of the appropriate volume for filtration should be based on extensive experience of the investigator. The optimal volume is a compromise between large enough volume that ensures large enough mass of particulate organic carbon on the filter and adverse effects that can arise from filtering large volume of water. These adverse effects can be associated, for example, with a long period of time (several hours) required to complete filtration of large volume and the possibility of unwanted effects on particles retained on the filter during the prolonged period of filtration (e.g., breakage of particles, lysis of biological cells). Upon the completion of filtration, the sample filters should *not* be rinsed with deionized water.

It is highly desirable to collect triplicate sample filters (or at least duplicate samples) to achieve an acceptable level of confidence in the final results.

9.2.3 Storage

Immediately following filtration, sample filters can be transferred to clean containers. Screw-cap glass scintillation-type vials are the preferred sample containers, but plastic petri dishes with lids or glassine envelopes are also acceptable. Wrapping filters in aluminum foil is acceptable, but not recommended as filters have a tendency to stick to the foil during drying. After filtration, the filters can either be dried in a drying oven (at 55 - 60°C until filter is completely dry) or kept frozen at < -20°C until post cruise analysis.

9.2.4 Blanks

A number of unused filters from a lot of precombusted filters are randomly selected as blanks. The blank filters are used to quantify background amount of organic carbon on filters and are processed identically to regular sample filters with the exception that the filtration of seawater sample is not applied. Although there is no specific recommendation for the number of blank filters, it should be adequate for providing statistically representative determination of the average blank value of organic carbon (taking at least 5-10 blank filters from a given lot of precombusted filters seems reasonable). Some investigators prepare dry filter blanks and others prepare filtered seawater blanks. Dry blanks represent just the pre-combusted GF/F filters which have not been exposed to any filtration process. Filtered seawater (FSW) blanks represent blank filters which have been exposed to filtration of pre-filtered seawater. The mass of background carbon on FSW blanks is typically higher by a few micrograms than on dry blanks. This difference is, however, smaller than the standard deviation of measurements taken on multiple dry or FSW blanks (Jennifer Massey, MSI Analytical Lab, UCSB, personal communication).

9.2.5 Analysis

The determination of POC is made with a standard CHN analyzer involving high temperature combustion of sample filters [*Parsons et al.*, 1984]. No specific commercially available analyzer is particularly recommended. As an example, a model CEC 440HA (manufacturer Control Equipment Corp., now

Exeter Analytical) is used at the Marine Science Institute (MSI) Analytical Lab, University of California Santa Barbara, which provides CHN analysis services for science community at a nominal fee per sample analyzed. Prior to combustion, removal of inorganic carbon can be done by fuming dried filter with concentrated hydrochloric acid (HCL) for 24h. Alternatively, ~0.25 mL of 10% v/v HCl can be applied directly to the sample filter. The acid-treated filters are re-dried at 55 - 60°C before combustion in the CHN analyzer. The blank filters are also treated with acid in the same way as the sample filters.

9.2.6 Calculation of Final Results

The final values of POC concentration are calculated by subtracting the average mass of organic carbon determined on blank filters from the mass of carbon determined on sample filters, and then dividing this result by the measured volume of filtered sample. Triplicate or duplicate POC samples are averaged to produce the final result of POC concentration.

9.3 Standard Accuracy/Error Analysis Criterion & Statistics Description:

9.3.1 Accuracy

The determination of accuracy of POC measured on marine samples is not straightforward, and no firm estimations of this accuracy exist. POC determinations are subject to several potential sources of errors that are difficult to accurately quantify and there is continued need for further research to improve the methodology and understand its accuracy [*Gardner et al.*, 2003]. Causes for potential positive bias (overestimation) of POC include:

- adsorption of dissolved organic carbon (DOC) onto filters during filtration.
- contamination of samples due to, for example, exposure to air during handling.

Other sources of error which can produce a negative bias (underestimation) of POC include:

- undersampling of rare large particles and incomplete retention of particles on filters.
- the loss of POC due to the impact of pressure differential on particles across the filters and other artifacts during filtration (e.g., breakage of fragile plankton cells).

9.3.2 Precision

The precision is defined as the reproducibility of a homogeneous standard or sample material (Kadar et al., 1993). Provided that a CHN analyzer is adequately calibrated and an appropriate standard is used, the precision of the analyzer is typically much higher than the variation observed for replicate marine samples. For example, for the CEC 440HA Elemental Analyzer used at the MSI Analytical Lab at UCSB, the precision is ±0.3% for carbon mass in the range 2 - 4000 µg. For marine POC samples, Stramski et al. [2008] reported the average coefficient of variation of 6% for replicate (mostly triplicate) samples from the eastern south Pacific and 5% for duplicate samples from the eastern Atlantic. Gardner et al. [2003] reported similar values.

9.3.3 Quality control

The procedures employed in the acquisition, storage, and analysis of POC samples should be reported in sufficient detail. Operation of a CHN analyzer should follow the optimal procedures established for a given instrument, which are typically described in sufficient detail in the manufacturer's manual. If

changes are introduced, these should be discussed with the manufacturer and other investigators using the same model of CHN analyzer.

A critical component of quality control is the reproducibility of replicate samples. It is recommended that the coefficient of variation of replicate samples should not exceed 10 - 15%. For such samples, the POC based on averaging the replicates can be accepted as validated data. If the coefficient of variation is higher than 15%, the results should be flagged as invalidated or lower quality data.

A useful index for quality control is the ratio of mass of carbon on blank filters to the mass of carbon on sample filters (i.e. blank-to-sample ratio). The lower the ratio the better quality of POC data is expected. Estimates of carbon on blank filters can be below the detection limit of a CHN analyzer (ideal scenario), but usually these estimates are above the detection limit. The blank values for 25-mm GF/F filters below 10 µg of carbon are considered typical and very good. For some filter lots, higher blank values between 10 and 20 µg are obtained. On rare occasions, even higher blanks are reported which may reduce significantly the quality of final POC data. With good blanks below 10 µg of carbon, it is relatively easy to achieve the blank-to-sample ratio below 10% for most oceanic waters by filtering sufficiently large volume of seawater. This is a desired result for this ratio. With higher blanks and samples collected in very clear hyperoligotrophic waters, this ratio can exceed 10%, however [*Stramski et al.*, 2008].

9.4 Parameter Accuracy Assessment and Rationale:

Category	Measurement Type							
	A	B	C	D	E	F	G	H
State of Art	x							
Quantitative	x							
Semiquantitative								
Research								

Define Measurement Type:

A: POC

9.5 Editorial note on Chapter 9

When this chapter was written, in 2010-2011 period, named approaches and references were considered state of the art. Current NASA community protocols on Particulate Organic Carbon are outlined in IOCCG series report by *Chaves et al.* [2021].

Chapter 10

Particulate Inorganic Carbon

William Balch, Bigelow Laboratory for Ocean Science, East Boothbay, Maine

10.1 Parameter Description:

Particulate inorganic carbon refers primarily to calcium carbonate concentration. It includes all mineral forms of calcium carbonate (e.g. common forms such as calcite and aragonite plus less common forms such as high-magnesium calcite, vaterite (rare), and ikaite (rare)). Given the focus on coccolithophores (which dominate the optical scattering in seawater due to their numerical abundance and high scattering cross section), calcite is the main mineral form.

10.2 Measurement Methodology Descriptions:

There are three types of measurements made in support of the PIC algorithm: analytical, IOP-based and AOP-based.

10.2.1 Analytical measurement

The most accurate PIC measurements are made using inductively-coupled plasma optical emission spectroscopy (ICP-OES). The basic technique for sampling involves filtration of 200-1000mL of seawater on 0.4um pore-size polycarbonate filters, rinsing with potassium tetraborate buffer (buffered to a pH of 8.0 to remove seawater calcium ions) then storage of the filters in ultra clean VWR trace metal clean, pp 15mL centrifuge tubes prior to analysis. PIC is then dissolved in ultra-clean 10% nitric acid, and analyzed using ICP-OES. This allows determination of the concentration of other elements in the sample, principally sodium, which allows for correction for any seawater contamination (which also carries 10 mM Ca^{++}).

10.2.2 IOP-based measurement

Underway measurements of PIC can be made using the above analytical technique but the expense of ICP-OES samples (~$14-16 per sample) makes this cost prohibitive for intensive surveys. Optical backscattering of PIC can also be used to estimate the standing stock of PIC. Acid-labile backscattering represents the backscattering that disappears following the lowering of seawater pH <5.8. This technique lends itself to semi-continuous measurements aboard ships, in which backscattering and pH are measured continuously in seawater from the ship's non-contaminated seawater system. Total particulate backscattering (b_{bp}) is first measured using a light scattering photometer. We sample the optical volume scattering function either using a Wyatt EOS volume scattering meter (which samples the VSF at 18 angles) or a WET Labs ECOVSF (which samples the VSF at 3 angles; this instrument is aimed into a sealed 2 L PVC chamber with angled end cap which helps reduce internal reflections). For the latter set-up, the wall-effect still can be observed and must be carefully be corrected-for using ultra-filtered Milli-Q water blanks. Every two minutes, the pH is lowered using a weak acid (glacial acetic acid) and PIC particles are dissolved as they traverse through a static mixer before the water enters the sensor volume. Once the pH *downstream of the optical sensor* stabilizes at <5.8, below the dissociation point for both aragonite and calcite, b_{bp} is re-measured. The difference between total and acidified b_{bp} represents "acid-labile backscattering" (b_b'). By using the same photometer for acidified and unacidified measurements,

Cite as: Balch, W. (2022), Particulate Inorganic Carbon, in PACE Technical Report Series, Volume 10: ACE Ocean Product Accuracy Assessments: A record of the state of the art circa 2010 (NASA/TM – 2022-219027/ Vol. 10), edited by I. Cetinić, C. R. McClain, P. J. Werdell and M. Behrenfeld, NASA Goddard Space Flight Space Center Greenbelt, MD

this eliminates inter-scatterometer calibration issues and causes only minor spatial aliasing in the b_b' measurement [*Balch et al.*, 2001].

Calcium carbonate also is highly birefringent (it rotates the plane of polarized light by 90^o), a property exploited by micropaleontologists for decades to enumerate biogenic and lithogenic mineral particles [*Haidar and Thierstein*, 2001]. This property also is being used along with automated image analysis techniques to identify and enumerate coccolithophores and detached coccoliths [*Balch and Utgoff*, 2009], even to estimate the amount of PIC in coccoliths [*Beaufort*, 2005]. The accuracy of this latter approach is still poorly constrained, however, and more work needs to be done.

A technique utilizing particle birefringence has been adapted to estimate PIC by adding polarizing filters to a transmissometer [*Guay and Bishop*, 2002]. It has been calibrated using purified mineral suspensions of diatomaceous earth and calcareous sediments. The technique shows promise. One possible limitation is that other organic molecules also can be highly birefringent. For example, in observations of thousands of samples with polarization microscopy, we have observed that zooplankton carapaces, certain dinoflagellate thecae as well as generic detritus can be birefringent [*Balch and Fabry*, 2008]. This would mean that in field samples, the presence of non-PIC, birefringent particles could potentially lower the accuracy of birefringence-based PIC estimates. Nonetheless, provided the above transmissometer technique is calibrated with suspensions of naturally-occurring particles (including naturally-occurring bifringent PIC *and* non-PIC particles), such errors should be easily quantifiable. This technology has been adapted for use on autonomous drifters [*Bishop et al.*, 2004], which provides useful information on the standing stock of PIC over the entire water column and at the mesoscale spatial domains, over periods of days to months. It would be especially useful for quantifying PIC in coccolithophore blooms.

10.2.3 AOP-based measurement

While optical scattering by PIC occurs in all directions (forward and backward), it is the strong backward scattering (b_b) of PIC that is critical to its being remotely sensed from above the ocean surface using spectraradiometers (either from ship, aircraft or satellite) [*Gordon et al.*, 1988]. For ship measurements, we use Satlantic SAS system with 7-wavelength radiance sensors for water and sky radiance measurements plus a spectral irradiance sensor (with cosine collectors, the same seven bands) for measuring spectral irradiance. Remote sensing reflectance at a given wavelength, λ, is a function of both absorption, $a(\lambda)$ and backscattering, $b_b(\lambda)$ and varies as $b_b(\lambda)/a(\lambda)$. Coccolith PIC has barely measurable absorbance [*Balch et al.*, 1991], thus the presence of PIC principally elevates b_b, thus increasing reflectance.

One complication in the optical remote sensing of PIC is that the relationship between $b_b(\lambda)$ or total integrated scattering ($b(\lambda)$) versus PIC concentration is not necessarily the same for different sized PIC particles. For example, optical scattering per unit PIC (otherwise known as the scattering cross-section, b* in units of m^2 $(\text{mole PIC})^{-1}$) is orders of magnitude lower for a large calcite particle like a pteropod than for a small coccolith [*Balch et al.*, 1996]. Moreover, the backscattering cross-section, b_b* shows moderate variability between different species of coccolithophores [*Balch et al.*, 1999]. This means that enhanced backscattering in the ocean caused by PIC is mostly due to small PIC particles like coccoliths *and is negligible for larger particles such as foraminifera and pteropods*. Moreover, this illustrates an important limitation of optical PIC determinations since the scattering cross-sections of small coccoliths are not constant but have some degree of variability, and layering of coccoliths, such as around cells, can cause nonlinear variability in their volume scattering properties.

Information on the backscattering cross-section of field PIC particles has been critical for development of coccolithophore remote sensing algorithms, which are fundamentally backscattering algorithms [*Balch et al.*, 2005; *Gordon et al.*, 2001]. The Gordon et al. [2001] three-band algorithm works best in turbid, bloom situations. This algorithm uses only bands in the red and near infrared (NIR) to minimize the influence of the absorption by chlorophyll and dissolved organic material. It incorporates published experimental determinations of the calcite specific backscattering and its spectral dependence, and assumes that the absorption coefficient of the medium was that of pure water, to estimate the marine contribution to the satellite-derived radiance. The aerosol (and Rayleigh-aerosol interaction) contribution to the radiance is modeled as an exponential function of wavelength. These allow derivation of the coccolith concentration on a pixel-by-pixel basis from ocean color imagery.

The two-band PIC algorithm [*Balch et al.*, 2005] is better suited to lower calcite concentrations. It is based on absolute values (not ratios) of 440nm and 550nm water leaving radiance and solves for chlorophyll and PIC based on their respective absorption and scattering properties. Natural variation in phytoplankton backscattering for chlorophyll concentrations < 10 mg/m^3 corresponds to a range of coccolith PIC of concentrations of 0-0.42 µM PIC. Thus, given accurate values of normalized water-leaving radiance, there will always be an uncertainty in coccolith concentrations of about 0.4 µM PIC at 1 kilometer resolution. The sensitivity of the radiances to coccolith concentration falls by about a factor of 2 from low to high chlorophyll concentration. The sensitivity when the chlorophyll concentration is > 2 mg m^{-3} is poor.

10.3 Standard Accuracy/Error Analysis Criterion & Statistics Description:

Analytical PIC estimate- The ICP-OES measurement of PIC has an accuracy of +/- 1nM. Given volumes filtered and 5:1 dilution in the digestion process, this translates to +/-5 to 20 nM PIC for 1000 and 200 mL filtrations, respectively.

IOP-based PIC estimate- Estimates of acid-labile backscattering, determined from field measurements have an error of +/- $5x10^{-5}$ m^{-1}. Due to the fact that the PIC-specific cross section of coccoliths is close to 1 m^2 $(mol\ PIC)^{-1}$, then this translates to an error of +/- $5x10^{-5}$ mol m^{-3} (=0.05 µmol L^{-1} PIC)

AOP-based PIC estimate- Histograms of ship and satellite-derived PIC concentration demonstrate similar concentration ranges in the Atlantic Ocean from 50°N to 40°S (i.e. bias<5%). Plots of satellite-derived PIC concentrations versus ship-based values are highly statistically significant (P<0.001), albeit they account for only about 63% of the total variance for a linear fit (SE +/-0.069umol L^{-1}). This result is to be expected, especially in oligotrophic waters in which there are other particles that affect the average background backscattering. In coccolithophore blooms, the relative precision of the PIC determination is higher due to the fact that PIC dominates all other particle backscattering (increased signal to noise). Along-track comparisons of satellite versus ship-derived PIC concentrations show regions of consistent satellite bias, probably associated with differences in water mass and particle types and mean changes in the background backscattering.

10.4 Parameter Accuracy Assessment and Rationale:

While remote-sensing algorithms for PIC are less precise than chemical PIC measurements, regional and temporal binning of satellite data allows time/space averages to be calculated with estimated standard errors well below the concentration of PIC in seawater [*Balch et al.*, 2005]. The error of the merged PIC algorithm for space/time scales of 1km and 1d is about 1.25 µmol PIC L^{-1} which exceeds the actual

concentration of PIC in the ocean. Assuming random error terms and zero bias, then the standard error of mean PIC estimates can be determined at different space/time binning scales. For example, at spatial scales of 4.6km and time binning of 8d, the standard errors of the PIC estimates are ~0.1 µM PIC L^{-1}, slightly less than the average global PIC concentration. For data binned over 36km and 30d, the standard error was 0.007 µM PIC L^{-1}, 1/16 of the average PIC concentration in the global ocean.

10.4.1 Quality assurance procedures

For analytical estimates of PIC, it is critical that filter handling be done in a clean manner, and that filters are well rinsed with potassium tetraborate buffer prior to storage. For IOP-based estimates of PIC (acid-labile backscattering), it is imperative that b_{bp} measurements of total and acidified samples be a) done with the same b_{bp} sensor and b) have sufficiently large sample size to reduce the SE, hence allow better discrimination of a small acid labile b_b signal. Typically, we average 60 individual samples in coastal waters (at 1Hz) and 90-120 samples in oligotrophic waters. Frequent calibration of b_{bp} sensors is also critical. For above-water AOP estimates of PIC, radiometric measurements should be made with well-calibrated instruments, measurements should be taken off the bow of the ship, far ahead of the bow wake, not subject to ship shadow. NASA Protocols for radiometric measurements should be stringently followed (including solar elevation limits, nadir and azimuthal viewing angles relative to the sun [*Mueller et al.*, 2003].

Category	**Parameter Classification**							
	A	B	C	D	E	F	G	H
State of Art	X							
Quantitative		X	X					
Semiquantitative					X			
Research				X				

A: Analytical PIC concentration

B: Acid labile backscattering

C: PIC merged two-band/three-band algorithm

D: Birefringence microscopy

E: Birefringence/transmissometer technique

10.5 Editorial note on Chapter 10

When this chapter was written, in 2010-2011 period, listed approaches and references were considered state of the art. An updated protocol was not available at the time of publication of this TM. Please check the IOCGG protocol document list at https://ioccg.org/what-we-do/ioccg-publications/ocean-optics-protocols-satellite-ocean-colour-sensor-validation/ regularly.

Chapter 11

Total Suspended Matter

Richard Stumpf, National Oceanic and Atmospheric Administration, Silver Spring, Maryland,

11.1 Parameter Description

Ocean: < 1 mg L^{-1}

Shelf/estuaries/river plumes: 2 - > 1000 mg L^{-1}

Suspended Particulate Matter (SPM) is the dry weight of particles in a unit volume of water. It is generally used to describe the inorganic component of the particulates. Several terms are used for this parameter, including suspended sediment, total particulate matter, total suspended material, and seston. While SPM includes both organic and inorganic materials, SPM becomes an important parameter in areas where inorganic material is a significant fraction of the particulate component. SPM is obviously of particular interest in coastal waters, where river plumes or resuspended sediments from the bottom are important. In case I water, SPM is generally uninteresting, as usually the particulates are better described by other information such as total phytoplankton, total calcite (from Coccolithophores), etc. In case 2 water, SPM may be important for estimation of various contaminants, or for identification of the amount of material that may deposit on important coastal habitats from river plumes or after storms. SPM strongly scatters light, so optical instruments that measure scatter, either beam transmissometers or backscatter sensors are used to estimate relative SPM.

11.2 Measurement Methodology Descriptions:

Standard SPM is potentially a simple measurement, but the standard is extremely sensitive to salt contamination, as the salt concentration in water may be 100-10,000 fold greater than the SPM. Accordingly careful treatment and rinsing of filters is critical to accurate measurements, as well as careful drying and humidity control. SPM from filters should be measured to accuracies of <0.1 mg per filter for glass fiber filters. In coastal waters, this equates to <10%; accuracies and precision of <5% are quite possible. In water with < 1 mg L^{-1} of SPM, accuracies (and the utility of the measurement), deteriorate rapidly unless large volumes of water are filtered. The problem is that a single large particle, such as a copepod, can significantly affect precision.

From an optical perspective, backscatter (b_b) or beam attenuation (c) provide an estimate of SPM, analogous to the relationship between $a_{\emptyset}$ and chlorophyll. If the particles are all of the same size and density, b_b can provide an accurate, nearly linear measure of the relative SPM [*Bunt et al.*, 1999]. Determination of absolute SPM requires calibration of the backscatter with measured SPM.

Other instruments are used to estimate SPM (such as the Coulter Counter and LISST, see the paper on "Particle Size Distribution"), however, these require assumptions about the particle characteristics, including shape and density.

Cite as: Stumpf, R. (2022), Total Suspended Matter, in PACE Technical Report Series, Volume 10: ACE Ocean Product Accuracy Assessments: A record of the state of the art circa 2010 (NASA/TM – 2022-219027/ Vol. 10), edited by I. Cetinić, C. R. McClain, P. J. Werdell and M. Behrenfeld, NASA Goddard Space Flight Space Center Greenbelt, MD

SPM has been measured from satellite using a variety of models, and it was characterized from space with the early Landsat satellites [e.g., *Stumpf*, 1988].

11.3 Accuracy and Precision:

As noted above, SPM from filters can be measured to <10%. While optical instruments can achieve highly stable and reproducible scatter measurements, conversion of backscatter (or the equivalent) to SPM is problematic. The key issue is determination of the specific backscatter, which is a function of the size and backscatter efficiency [*Baker and Lavelle*, 1984]. Backscatter can be measured accurately from satellite, particularly in near-infrared (NIR) wavelengths [*Ruddick et al.*, 2006]. Conversion to SPM on a global scale requires the accuracy of the backscatter determination in the NIR. Determination of SPM in any region requires a correction for variations in particle characteristics [*Bowers and Binding*, 2006; *Forget et al.*, 1999]. While a single relationship may generally apply to a large region, wind or storm events may alter the relationship by a factor of two [*Stumpf*, 1988]. In most cases the absolute SPM can be achievable locally to a factor of 2, with relative SPM being accurate to the accuracy of backscatter and the calibration relationship. A global algorithm may have local accuracy of only an order of magnitude [*Babin et al.*, 2003]. Precision for local regions will be superior under average conditions, but not during resupension events [*Woodruff et al.*, 1999].

11.4 Parameter Accuracy Assessment and Rationale:

Category	**Measurement Method**							
	A	B	C	D	E	F	G	H
State of Art								
Quantitative	X							
Semiquantitative			X					
Research		X						

A: Filtered SPM

B: Coulter Counter, Laser In-situ Scattering and Transmissometry (LISST by Sequoia Scientific)

C: Optical (backscatter or transmissometer)

11.5 Editorial note on Chapter 11

When this chapter was written, in 2010-2011 period, listed approaches and references were considered state of the art. An updated protocol was not available at the time of publication of this TM. Please check the IOCGG protocol document list at https://ioccg.org/what-we-do/ioccg-publications/ocean-optics-protocols-satellite-ocean-colour-sensor-validation/ regularly.

Chapter 12

Carbon and Chlorophyll-to-Carbon Ratios

Michael Behrenfeld, Oregon State University, Corvallis, Oregon

12.1 Parameter Description:

What is the contribution of phytoplankton carbon standing stock to total particulate organic carbon in the sea? How variable is this contribution? How do physical climate forcings, such as ENSO cycles or ocean basin decadal oscillations, influence the biomass versus physiological status of phytoplankton? How similar or dissimilar are magnitudes of phytoplankton blooms in the various seasonal seas of the global ocean? These and other first-order questions regarding phytoplankton ecology and ecosystem structure and function can not be adequately assessed through observations of upper ocean chlorophyll concentrations. What is required instead is the direct assessment of phytoplankton carbon concentration (Cphyt).

A key complication in the interpretation of chlorophyll data is that pigment concentration is a function of both phytoplankton standing stock and physiological state. The physiological component of this equation reflects changes in intracellular chlorophyll levels associated with nutrient-driven changes in phytoplankton growth rates and variability in the light level to which phytoplankton are acclimated. The natural range in these two environmental forcing (light and nutrients) can drive variability in phytoplankton pigmentation over a range of one and a half orders of magnitude, which is comparable to variability in phytoplankton standing stocks. However, while physiological plasticity compromises the utility of chlorophyll concentrations as a reasonable proxy of biomass, it also endows chlorophyll data with critical information on physiology that can be retrieved if measured in concert with an independent index of Cphyt. In other words, the simultaneous collection of chlorophyll and Cphyt data is a powerful combination that provides insight on both variations in standing stocks and physiological status, the later through variability in the C:Chl ratio.

12.2 Measurement Methodology Descriptions:

There are no routine field techniques for measuring carbon or C:Chl for the entire phytoplankton community in a given assemblage. Some investigators have analyzed variability in the chlorophyll to total particulate organic matter (POC) ratio, but this approach does not account for variability in the non-phytoplankton contribution to POC. Other investigations have estimated phytoplankton carbon from chlorophyll by either assuming a constant Chl:C ratio or by attempting to correct for physiological effects of light and nutrient stress. Such approaches are also unsatisfactory in that they either neglect the significant role of physiology in chlorophyll variability or do not fully account for this physiological component. The most direct approaches for assessing phytoplankton biomass entail enumeration and sizing of phytoplankton, followed by calculation of carbon through assumed C:volume relationships (with the occasional addition of including corrections for different phytoplankton shapes). In addition to uncertainties in these conversion factors, there are multiple technical and practical issues with this approach. One important issue is that no instrument has yet been developed that can adequately sample the entire phytoplankton size domain. Instead, the smallest phytoplankton size fraction is characterized using one technique (e.g., flow cytometry or epifluorescence microscopy) and the larger size fraction is

Cite as: Behrenfeld, B. (2022), Carbon and Chlorophyll-to-Carbon Ratios, in PACE Technical Report Series, Volume 10: ACE Ocean Product Accuracy Assessments: A record of the state of the art circa 2010 (NASA/TM – 2022-219027/ Vol. 10), edited by I. Cetinić, C. R. McClain, P. J. Werdell and M. Behrenfeld, NASA Goddard Space Flight Space Center Greenbelt, MD

characterized using a different technique (e.g., light microscopy or optical imaging), and then an attempt is made at merging the two data sets to give total phytoplankton carbon. For many of these techniques, the sample volume analyzed is exceeding small, raising issues of representativeness. In addition, microscopic analyses are extremely labor intensive, require sample preservation, and often require sample filtration, which introduces additional errors/uncertainties. Reflecting the difficulty of these assessments, the historical record of phytoplankton carbon estimates pales in comparison to the relatively numerous assessments of phytoplankton pigment concentrations or carbon fixation rates.

12.3 Standard Accuracy/Error Analysis Criterion & Statistics Description:

There is no standard material for natural, mixed-community phytoplankton carbon biomass. However, standard beads are used in flow-cytometric systems for calibration of retrieved particle volumes. In the laboratory, phytoplankton carbon-to-volume relationships have been derived for a variety of culture species. Under such condition, phytoplankton carbon can be assessed through filtration and analysis with a CHN analyzer. Uncertainties in CHN measurements are thoroughly discussed in the accompanying Parameter Assessment for POC by Dariusz Stramski. An additional complication for the laboratory phytoplankton carbon assessment is quantifying the contribution of contaminating bacteria. This issue, however, is minimized when measurements are conducted using 'axenic' cultures. Uncertainties in field-derived C:Chl ratio are also introduced through uncertainties in chlorophyll assessments. These uncertainties are discussed in detail in the accompanying Parameter Assessment for pigments by Standford Hooker.

12.4 Parameter Accuracy Assessment and Rationale:

The accuracy of field phytoplankton carbon and C:Chl estimates is currently unquantified

Category	**Parameter Classification**							
	A	B	C	D	E	F	G	H
State of Art								
Quantitative								
Semiquantitative								
Research	X	X						

A: Phytoplankton Carbon

B: Phytoplankton Carbon:Chlorophyll

12.5 Editorial note on Chapter 12

When this chapter was written, in 2010-2011 period, listed approaches and references were considered state of the art. An updated protocol was not available at the time of publication of this TM. Please check the IOCGG protocol document list at https://ioccg.org/what-we-do/ioccg-publications/ocean-optics-protocols-satellite-ocean-colour-sensor-validation/ regularly.

Chapter 13

Particle Size Distributions

Tiho Kostadinov and David Siegel, University of California Santa Barbara, Santa Barbara, California

13.1 Parameter Description

The differential particle size distribution is effectively a histogram N(D) of particle number counts in a given volume of water over some specified size bins of nominal diameter D. The bins have effective edges and widths and are usually logarithmically spaces in theoretical considerations and practical instrumental measurements. The SI units of N(D) thus become m^{-4}, because the bin particle counts per unit volume of water are normalized to the bin width. N(D) is usually modeled as a power law,

$$N(D) = N_o (D/D_o)^{-\xi}$$

where ξ is the power-law slope of the PSD, N_o is the number concentration at a reference diameter (D_o). The total number of particles can be calculated by integrating N(D) over the range of applicability (e.g. *Kostadinov et al.* [2009]). This requires that the limits of N(D) be considered.

In practice, available instrumentation for particle sizing in the size range of interest to optics allows for measurements from 1-3 μm of diameter to about 250-500 μm with the same instruments (described below). Most measured PSD's fit reasonably well to the power-law, and bounds on the variability in ocean water are as follows:

ξ: 2.5 – 6 (dimensionless)

N_o: 10^{13}-$10^{17.5}$ m^{-4} for D_o = 2 μm.

13.2 Measurement Methodology Descriptions:

There are two major commercially available instruments used in the field today that measure particle size in the range of interest to ocean optics. First, the Coulter Counter is a widely used instrument based on changes in the electrical current passing through an orifice as particles suspended in an electrolyte are passed through the orifice. As such, the instrument is sensitive to particle cross-sectional area, because the area of the displaced electrolyte in the orifice is proportional to current changes. The raw output of the Coulter Counter is particle numbers in the specified size bins, which depend on the orifice chosen. Coulter counter observations are difficult due to frequent blockages of the orifice – especially when small orifice sizes are used.

Second, a newly developed instrument based on laser diffraction principles is gaining popularity, the LISST (Laser In-situ Scattering and Transmissometry) by Sequoia Scientific (http://www.sequoiasci.com/products/fam_LISST_100.aspx). A red laser is shone upon a sample volume and 32 concentric sensor rings detect scattering in near-forward angles. This scattering is due to diffraction and is therefore not sensitive to the internal composition of particles. This allows the application of Mie theory (with the assumption of sphericity and homogeneity) to invert for the PSD that would have produced that scattering pattern. The LISST actually measured the near-forward volume scattering function (VSF). The raw output is laser power detected in the 32 rings, which is then inverted

Cite as: Kostadinov, T and D. Siegel (2022), Particle Size Distribution, in PACE Technical Report Series, Volume 10: ACE Ocean Product Accuracy Assessments: A record of the state of the art circa 2010 (NASA/TM – 2022-219027/ Vol. 10), edited by I. Cetinić, C. R. McClain, P. J. Werdell and M. Behrenfeld, NASA Goddard Space Flight Space Center Greenbelt, MD

by the manufacturer's software to particles volumes (μL/L) in each of the 32 logarithmically spaced size bins., ranging from 1.25 μm to 250 μm in the case of the type B LISST-100X. The LISST is actually sensitive to particle effective cross-sectional area for scattering, even though its output is given as volume concentrations.

13.3 Accuracy and Precision:

It is not trivial to quantify the accuracy of PSD measurements from either instrument described above. Several sources of uncertainty propagate to the estimated parameters, e.g. the PSD slope ξ and N_o. The uncertainty will be therefore different depending on the desired variable, e.g. total concentration in the entire size range vs. the concentration is a specific size range vs. the PSD slope. Additionally, the Coulter Counter and the LISST are based on very different principles, so their sources of uncertainty are different. Coulter counter accuracy is reported as aperture current accuracy (e.g. 0.4% of setting for the Beckman Multisizer 4[1]), which needs to be translated to the actual variable of interest statistically. The main sources of Coulter counter counting uncertainty are the coincidence problem at small diameters and statistical bias at large ones[2] [*Milligan and Kranck*, 1991]. Analyzing additional sources of error, such as the edge effect (particle asses near edge of orifice), the shape effect (particle is non-spherical) and the particle resistance error (different resistance as compared to the calibrating particles), *Boyd and Johnson* [1995] conclude that diameter estimate error can be up to 14%, which reduces the effective bins to ~17 for live marine samples that include non-spherical phytoplankton.

Regarding the LISST, specific accuracy/precision estimated are not given[3]. However, the LISST software regards any bin concentrations smaller than 0.001 μL/L as negligible and sets them to 0 μL/L (O. Mikkelsen, pers. comm.), so this number can be accepted as a lower bound on the accuracy. Additional sources of uncertainty for the LISST include particle non-sphericity (the inversion assumes spherical particles). Sequoia now provides a separate inversion matrix for randomly shaped particles which results in different concentrations and different bin sizes. The assumption of sphericity when the particles are random can result in an overestimation of particle size [*Agrawal et al.*, 2008]. An on-going issue with the LISST are data at 'edges' in the PSD, i.e. at the small and large extremes of the PSD, the LISST exhibits large deviations from the power-law approximation which appear to be artifacts, due for example to 'leakage' of scattering by particles outside of the measured range. For this reason, some investigators disregard several bins on each end of the PSD (Heidi Dierssen and Emmanuel Boss, pers. comm.). This scheme can be applied to the Coulter Counter as well.

13.3.1 Quality assurance procedures

Coulter counter:

-calibrations of the aperture with blank samples and known particles sizes.

LISST:

[1] Beckam Coulter, Inc. (2008), User's Manual Multisizer 4 Particle Analyzer. Fullerton, CA
[2] Sheldon, R. W., and T. R. Parsons (1967), A practical manual on the use of the Coulter Counter in marine science, report, Coulter Electron, Toronto, Ont., Canada.
[3] Sequoia Scientific, Inc. (2009), LISST-100X Particle Size Analyzer User's Manual Version 4.65. Bellevue, WA.

-pure water calibrations before each sampling day to ensure instrument is aligned and laser power is within factory specified limits for particle-free water.

-averaging repeat measurements over longer time (e.g. a minute)

-running known particle sizes through the LISST as verification.

13.4 Standard Accuracy/Error Analysis Criterion & Statistics Description:

Agrawal and Pottsmith [2000] found laboratory tests of the LISST with 30 µm bins to be satisfactory against NIST standards; they also provide the volume conversion constant for the LISST. Independent laboratory tests with standard beads indicate the LISST correctly sizes particles to within 2-18% of their diameter (LISST underestimates diameter and error increases with particle size); however, the volume conversion constant was found to vary over a factor >3 with particle size [*Gartner et al.*, 2001]. However, *Traykovski et al.* [1999] found that the LISST slightly overestimated natural sediment sizes and that the LISST is capable of retrieving total volume concentrations correctly with a single calibration constant as long as the linearity range of the instrument is observed. *Mikkelsen et al.* [2005] find large errors in total volume determinations. Kostadinov et al. (unpublished data) find excellent agreement between LISST volume concentrations and independent POC determinations in the Santa Barbara Channel. *Slade and Boss* [2006] calibrated the LISST with beads of known diameter in order to measure near-forward VSF and found a realistic upper bound on the VSF error to be ~30% on average. *Buonassissi and Dierssen* [2010] found satisfactory agreement between the LISST and the Elzone particle counters, except where the LISST exhibited the artificial tail at the edge of the distributions.

Regarding the size resolution of the LISST, Sequoia Scientific (2008) [4] report that noise in the data and mathematical properties of the inversion problem limit the resolvable size bins to 10-12 (e.g. across the 1.25 – 250 µm particle diameter measurement range of the type B instrument), even though there are 32 detector rings and size bins solved for. This is roughly consistent with the results of *Traykovski et al.* [1999] who report that the LISST is capable to resolve bimodal PSD's if the mean diameters of the modes are at least a factor of two apart.

Coulter counters are calibrated with standardized beads, which are spherical and generally have different electrical resistivity as compared to living cells. When the Coulter counter accuracy and precision are assessed against electron microscopy of various bead standards, excellent results are obtained. In general, differences in mean diameter estimated from the Coulter counter and electron microscopy is less than 5% (e.g. *Alliet* [1975]). However, as summarized above, *Boyd and Johnson* [1995] assessed Coulter counter accuracy for natural marine particles and found that 1) due to the 'edge error' (particle passing closer to the edge of the orifice) particle volume can be overestimated by 16-20% (diameter error of ~5%); 2) certain preservation techniques can render fixed cells electrically transparent, resulting in severe underestimation of volume (~70%); 3) a small volume underestimation of ~3-5% can result due to different resistivity of the calibration standard and the sample; 4) the shape factor error can introduce an additional error of ~25% in volume estimation, which can lead to a combined volume estimation error of ~40% (~14 % in equivalent spherical diameter). This can cause cell size and biomass to be underestimated by up to 25% if primarily elongated particles are counted. They conclude that only ~17

[4] Sequoia Scientific, Inc. (2008), The size resolution of the LISST series of instruments, http://sequoiasci.com/Articles/ArticlePage.aspx?pageId=120 (Retrieved July 7, 2010)

useful size spectrum channels are obtainable with the Coulter counter for natural non-spherical marine particle samples.

Finally, it is worth noting that the LISST samples in-situ, whereas the Coulter counter tends to destroy delicate particle aggregates, which can introduce a bias in the PSD estimate.

13.5 Parameter Accuracy Assessment and Rationale:

Category	Measurement Method							
	A	B	C	D	E	F	G	H
State of Art								
Quantitative	x	X						
Semiquantitative								
Research								

Define Measurement Type

A: Coulter Counter

B: Laser In-situ Scattering and Transmissometry (LISST by Sequoia Scientific)

13.6 Editorial note on Chapter 13

When this chapter was written, in 2010-2011 period, listed approaches and references were considered state of the art. An updated protocol was not available at the time of publication of this TM. Please check the IOCGG protocol document list at https://ioccg.org/what-we-do/ioccg-publications/ocean-optics-protocols-satellite-ocean-colour-sensor-validation/ regularly.

Chapter 14

Trichodesmium Abundance

Toby Westberry, Oregon State University, Corvallis, Oregon

14.1 Parameter Description

Trichodesmium is a genus level distinction of a colony-forming, nitrogen-fixing, photosynthetic cyanobacteria. *Trichodesmium* has historically been the most conspicuous and most important marine diazotroph in oceanographic studies. Its role in biogeochemical cycling and its unique optical characteristics have also made it the target of several bio-optical and remote sensing studies [*Borstad et al.*, 1992; *Subramaniam et al.*, 2001; *Westberry et al.*, 2005]. More than one related abundance index is often reported in the literature due to this organism's morphology in which individual cells are concatenated into long filaments (or trichomes), and which are further bundled into colonies. Number of cells per trichome and trichomes per colony is highly variable, and both free trichomes and colonies are found in field samples. Common practice in the field is to disaggregate colonies and enumerate individual trichomes.

Relevant units are colonies m^{-3} or trichomes L^{-1}. The range in the surface ocean is from $0\text{-}10^4$ trichomes L^{-1} with rare surface blooms (almost exclusively coastal phenomenon) reaching $>10^6$ trichomes L^{-1}. Representative values of ~200 trichomes per colony and ~100 cells per trichome are often used for conversion between units, but these values can also be highly variable.

14.2 Measurement Methodology Descriptions:

The preferred method of sample collection in the field is via gravity filtration of a full Niskin (or GoFlo) bottle (~10L) on to a 10µm Nuclepore (or similar) filter. An inline filter holder can be connected directly to the spigot of the Niskin bottle in order to minimize disturbance to colonies. Filters can be preserved if needed with 2% Para-formaldehyde and mounted on oversize microscope slides with non-fluorescent immersion oil [*Carpenter et al.*, 2004; *Letelier and Karl*, 1996]. Subsequent quantification of *Trichodesmium* abundance is carried out using epifluorescence microscopy and phycoerythrin autofluorescence. Conversion of counts into a concentration is similar to any microscopy-based counting technique (e.g., *Sherr et al.* [1993]and assuming the area counted is one field of view):

$$\#/L = \frac{(cells/\ field\ \ of\ view) \times (area\ of\ \ filter\ \mathrm{cov}ered\ by\ sample)}{(field\ of\ view\ area) \times (liters\ \ filtered)}$$

Automated methods using simple image processing techniques have also been developed [e.g., *Kovesi*, 1999]. In this case, a recording device (camera) is mounted to the ocular of the epifluorescence microscope to record and store the images. The rectilinear shape of trichomes and their well-constrained width allow easy assessment of total area of an image covered by trichomes which can be divided by the width to yield number of cells [e.g., *Hynes*, 2009].

Cite as: Westberry, T. (2022), Trichodesmium Abundance, in PACE Technical Report Series, Volume 10: ACE Ocean Product Accuracy Assessments: A record of the state of the art circa 2010 (NASA/TM – 2022-219027/ Vol. 10), edited by I. Cetinić, C. R. McClain, P. J. Werdell and M. Behrenfeld, NASA Goddard Space Flight Space Center Greenbelt, MD

It should also be pointed out that much of the *Trichodesmium*-related literature does not report abundance, *per se*. Most physiological studies in the field require concentrations of these organisms above that found in the water column. Therefore, a plankton net with ~100µm mesh is towed for some duration and the individual colonies are hand-picked from the cod end of the net, washed with sterilized seawater and isolated for further processing. These studies generally do not provide adequate measures of abundance.

Taxonomy of *Trichodesmium* is complicated and very fluid. Many of the species and even other genus have been recently reclassified (e.g., Katygnemene). Prevailing morphologies and coloration (a variety of phycobilliproteins exist amongst species) may be a function of physiological status as much as taxonomy.

14.3 Standard Accuracy/Error Analysis Criterion & Statistics Description:

Uncertainties associated with this parameter arise both from sampling biases as well as errors imparted by the individual operating the microscope. A round-robin type intercalibration was carried out in 2005 to assess uncertainty due to the latter [*Vuorio et al.*, 2007]. Although the study was not focused on *Trichodesmium* specifically, two of the three taxa used were filamentous (trichome forming) cyanobacteria, *Planktothrix* and *Anabaena,* and thus, should be relevant. The reported coefficients of variation (CV), based on 14 different individual scientists' counts of **cells,** were 20% and 18% for these two species, respectively. CV's for **trichome** counts were 13% and 23% for *Planktothrix* and *Anabaena,* respectively. Variability within subsamples counted by a single scientist were as high as 20%, and even higher, up to 57% between different analysts.

14.4 Parameter Accuracy Assessment and Rationale:

Category	**Measurement Type**							
	A	B	C	D	E	F	G	H
State of Art								
Quantitative								
Semiquantitative	X							
Research								

A: Trichodesmium abundance

14.5 Editorial note on Chapter 14

When this chapter was written, in 2010-2011 period, listed approaches and references were considered state of the art. An updated protocol was not available at the time of publication of this TM. Please check the IOCGG protocol document list at https://ioccg.org/what-we-do/ioccg-publications/ocean-optics-protocols-satellite-ocean-colour-sensor-validation/ regularly.

Chapter 15

Primary Production

Margaret R. Mulholland, Old Dominion University, Norfolk, Virginia

15.1 Parameter Description

Net Primary Production (NPP) generally describes the net fixation of dissolved inorganic carbon (DIC) into algal (or plant) biomass and translates into growth. Some fraction of DIC that is taken up is not incorporated into biomass but is either released as dissolved organic carbon (DOC) or is respired. As stated by Behrenfeld, NPP "represents the rate of photosynthetically-generated organic matter production". To estimate NPP in nature, methods employ measurements of the common elements in the photosynthetic equation (e.g., oxygen (O) and carbon (C), and even nitrogen (N)). The most common method for estimating NPP is the ^{14}C uptake technique (described by Behrenfeld). An alternative method that can be employed in the same ways as described above is the ^{13}C uptake technique. An advantage of this technique is that it relies on a stable isotope of C and therefore there are fewer restrictions on its use aboard ships or in the laboratory. Disadvantages of the ^{13}C method are that it requires an isotope ratio mass spectrometer (IRMS) to measure the isotope ratio at the end of experiments and it requires additional measurements; the initial and final concentrations and isotopic compositions of the particulate organic carbon (POC) and DIC pools.

In general, isotopic tracers are used to provide direct estimates of the movement of elements from one pool to another. In the simplest application, two relevant pools are considered; some source pool from which the element is removed (in this case DIC) and a target pool into which the element accumulates (plant biomass). A two-component mixing model can then be used to calculate the one-directional transport of the element from one pool to the other. When using stable isotopes to calculate transfer of material between pools one must know something about the size and reactivity of the source and target pools, their natural isotopic signatures, and the relevant timescales for the processes of interest.

The problems associated with experimental design will not be covered in detail here. Basically, one must decide on the materials to be used in a tracer study (e.g., types of bottles, filters, etc.), the amount of a tracer addition (usually depends on the concentration of the source pool and sensitivity of instrumentation), the amount of material that must be collected at the beginning and end of a experiments needed to make accurate measurement for both source or target pools (usually depends on instrument sensitivity and the concentrations of the source and target pools), and the length of the incubation (depends on the reaction rate and sensitivity of instrumentation). For primary productivity estimates, light and dark bottles are used for incubations (these can be the same types as those used for ^{14}C incubations). Incubations are generally 12 or 24 hours (as for ^{14}C), after which samples are collected onto precombusted (450°C for 2 h to remove contaminating C) GF/F filters (nominal pore size 0.7 □m) or other glass fiber filter, or silver filters that are available in various pore sizes. DIC concentrations can be measured directly or calculated. A 10% tracer addition is generally considered best so as not to conduct a perturbation experiment but yet achieve sufficient sensitivity. Tracer additions < 1% often yield spurious results and should be avoided [*Mulholland et al.*, 2009].

Cite as: Mulholland, M. R. (2022), Primary Production, in PACE Technical Report Series, Volume 10: ACE Ocean Product Accuracy Assessments: A record of the state of the art circa 2010 (NASA/TM – 2022-219027/ Vol. 10), edited by I. Cetinić, C. R. McClain, P. J. Werdell and M. Behrenfeld, NASA Goddard Space Flight Space Center Greenbelt, MD

Field data describing ^{13}C uptake results can be expressed in the same units as for the ^{14}C method, volumetrically (mmol C/L/day or mg C/m^3/day) or areally (mmol C/m^2/day or mg C/m^2/day). However, the terminology used in stable isotope calculations can be confusing and is different from that used for radioisotopes. For radioisotopes, radionuclides undergo decay and this decay is measured directly and related to the specific activity or the rate of decay per unit mass of an element. Radioisotopes can be added at very small concentrations and, because radioisotopes are very sensitive, perturbations to the source pool have been thought to be negligible. Movement from that source pool into a target pool can be measured by measuring the radioactivity in that pool after some time. For stable isotopes, there is no nuclear decay, rather instruments measure the ratios of ^{13}C/(total C) in a particular source or target pool (see Equation 1 below) of at the beginning and at the end of incubations.

Using stable isotopes as tracers is mathematically less direct than using radioisotopes because the output of isotope ratio mass spectrometers is a ratio rather than an absolute value. Consequently, to calculate rates from stable isotopes, we also need to know something about the concentrations or amounts of the different isotopes of an element in nature and their isotopic signatures.

15.2 Measurement Methodology Descriptions:

A method for measuring photosynthesis using ^{13}C was first described by *Slawyk et al.* [1977] but this relied on incorrect simplifications made to the ^{15}N uptake equations outlined above. The correct equations were outlined in *Fisher Jr et al.* [1979]. For C, it is very important to measure or have a good estimate of the initial isotopic signature of the PC pool because this can vary widely among systems. For example, phytoplankton can range from ^{13}C values of 0 to –40. Similarly, the DIC or other C source pools can vary widely depending on factors affecting the addition or removal of material from the pool and fractionation during recycling processes.

15.2.1 Long-term Measurements

Protocols for long-term ^{13}C measurements are similar to those described for ^{14}C. The rate of carbon fixation is measured by tracing the uptake of ^{13}C from DIC into particulate organic carbon (POC) and the uptake is calculated using a two end-member mixing model. A known amount of highly enriched (95-99%) ^{13}C-labeled bicarbonate is added to “enrich” the dissolved inorganic carbon pool by roughly 10%. The atom percent (atm %) refers to the % ^{13}C in a particular pool such that:

$$\text{Atm \% } ^{13}C = \frac{^{13}C}{(^{13}C + ^{12}C)} * 100 \qquad (1)$$

where $^{13}C + ^{12}C$ is the total C pool (other isotopes of C are not considered). This can be in terms of atoms or mass.

The atm % enrichment of the DIC pool is calculated as follows:

$$\text{atm \% enrichment DIC} = \frac{(\text{Atm \% DIC} * [\text{DIC}])_{\text{ambient}} + (\text{Atm\% DIC} *[\text{DIC}])_{\text{tracer}}}{[\text{DIC}]_{\text{ambient}} + [\text{DIC}]_{\text{tracer}}} \quad (2)$$

Either the concentration or amount (e.g., either µg, µmol or µM) can be used in this equation but, whichever is chosen, all of the calculations should be done in the same units.

C uptake is calculated from the enrichment of the DIC pool at the beginning of the experiment, and the enrichment of ^{13}C in the POC pool at the end of the incubation relative to the natural abundance of ^{13}C in the POC pool at the start of the experiment, using a mixing model [see *Montoya et al.*, 1996; *Mulholland et al.*, 2006] as follows:

$$\text{DIC Uptake} = \frac{(\text{atom \% PC})_{\text{final}} - (\text{atom \% PC})_{\text{initial}}}{(\text{atom \% enrichment DIC} - \text{atom \% PC})_{\text{initial}} * \text{time}} \text{ x [POC]} \quad (3)$$

Major assumptions incorporated into the use of this equation are that the isotope from the source (DIC) pool is moving in one direction (into the target PC pool) and the source and target pools are not affected by any other reactions. If this is not true then some additional corrections can be made to the calculation. In addition, this equation assumes that the atom % of the source pool doesn't change significantly over the course of an incubation, which may not be accurate if there is DIC production in the incubation bottle. Modification of these calculations can be made to account for isotope dilution over the course of the incubation.

The measurement of the ratio of $^{13}C/^{12}C$ in particulate matter is typically done using an isotope ratio mass spectrometer. There are several manufacturers of appropriate instruments and many configurations for the inlet to these instruments. Reviews of this instrumentation can be found in *Boutton et al.* [1991] and *Fiedler and Proksch* [1975]. In general, isotope ratio mass spectrometers have gas inlet lines and are equipped with two or more ion beam collectors to collect two or more ion beams of different masses. The element of interest must be isolated from its matrix, and converted to a stable gas that can be introduced into the IRMS. Nitrogen and carbon analyzers are commonly interfaced at the inlet to allow combustion of particulate samples and measurement of C and N mass on the same sample introduced into the IRMS. Dual inlet IRMS systems allow sample and reference gas to be compared repeatedly throughout sample runs.

For C, samples are analyzed as CO_2 and so ion masses of 44, 45 and 46 are compared. The $^{13}C/^{12}C$ ratio is calculated from a combination of mass 45/44 and mass 46/44 ratios and corrected for minor ^{17}O contributions to the mass 45 signal.

Stock ^{13}C sodium bicarbonate is available from a variety of vendors. A sodium carbonate (anhydrous) solution is prepared in an opaque, acid-cleaned teflon or other plastic nutrient bottles. The ^{13}C stock is

stored refrigerated (5°C) or frozen until use. Some labs recommend further purification of the stock solution to remove any residual trace metal contamination.

For each experiment, seawater sample is dispensed into polycarbonate or other inert plastic or glass incubation bottles. Bottles are rinsed 3 times with seawater samples prior to being filled. New bottles are soaked for 72 hours in seawater. Bottles are then rinsed thoroughly with deionized water, and subsequently soaked for 72 hours in the acid cleaning solution. The acid is discarded and the bottles rinsed with Milli-Q water and then soaked in Milli-Q for at least 48 hours. Once a new bottle has been cleaned as described above, then cleaning between cruises consists of soaking in the acid cleaning solution for several days and rinsing 3 times with Milli-Q before use.

The same sampling considerations outlined for ^{14}C incubation experiments apply for ^{13}C incubation experiments. As for ^{14}C, additional dark bottle(s) incubation is (are) included to assess non-photosynthetic carbon uptake. Following incubation, samples are collected and filtered typically onto pre-combusted (450ºC for 2 h) 25 mm Whatman GF/F glass fiber filters under low vacuum (70 mm Hg or less) and low background light levels. Sample are rinsed 3 times with artificial or filtered seawater to removed adsorbed isotope. Filters are then placed into sterile cryovials and stored frozen until analysis. To prepare samples for analysis using an IRMS interfaced with an elemental analyzer preparation unit, samples are dried in an oven at 60ºC and then pelletized into tin disks and placed in 96 well trays and stored dry (in a desiccator) until analysis. NPP is calculated by subtracting the dark bottle DIC uptake from the light bottle DIC uptake.

15.2.2 Isotopic discrimination

Inherently, both ^{14}C and ^{13}C calculations assume that the source pool is completely reactive and that the process being measured does not isotopically fractionate (in practice, a fractionation factor is often included in the calculation of photosynthesis because this process does fractionate). It also assumes that photosynthesis is the only process affecting the DIC pool or that turnover of the DIC pool is related only to photosynthesis.

15.3 Standard Accuracy/Error Analysis Criterion & Statistics Description

15.4 Parameter Accuracy Assessment and Rationale

The measurement of primary production generally has no independent method for calibration. Intercomparison of techniques is also difficult without explicit activities on the same ship or same station. Data are generally evaluated for “reasonableness” in the context of other measurements in the area or other measurements made by a given investigator. The precision of the isotope ratio measurement is high, much higher than that for the mass of particulate C.

In addition to the factors that influence accuracy of ^{14}C uptake measurements in estimating NPP, there are some other factors that influence the accuracy with which ^{13}C uptake measurements estimate in situ NPP. Particulate samples are not acidified prior to their analysis as this could interfere with isotopic analysis, consequently PC can include inorganic carbon as well as detrital carbon. This can yield overestimates in PC and specific uptake rates as they are directly proportional to PC. Unlike ^{14}C measurements, which track DIC into the particulate pool, ^{13}C calculations also incorporate information about the particulate C pool. One can calculate the absolute amount of ^{13}C in the particulate pool (or any target carbon pool) by simply multiplying the atom% (after dividing by 100) by the target pool concentration

To relate the atom % to the mass or concentration of ^{13}C in a sample, one can calculate:

$$[^{13}C]_{pool} = (\text{atom } \%_{pool}/100)*[\text{C concentration or mass}]_{pool} \quad (4)$$

What mass spectrometers actually measure is the abundance of $^{44}CO_2$, $^{45}CO_2$ and in some cases $^{46}CO_2$. Software used to collect data from mass spectrometers can be programmed to output data in terms of the ratio (R) of (mass 45)/(mass 44) for C. The atom % is $[^{13}C]/[^{13}C+^{12}C]$ times 100 where the denominator is assumed to be equal to the total C in the pool measured), or in a differential or delta notation which is a comparison with a standard reference material (for C this is the PeeDee belemite). Standard reference materials are available through NIST. One must first know the units that the instrument is programmed to report data in and then be able to relate these numbers to the atom percent of ^{13}C in an environmental or enriched sample.

To relate isotopic compositions absolutely, one usually reports isotopic ratios in differential or delta notation. However, for tracer studies, comparisons are made between "enriched" and "unenriched" samples or changes in relative enrichment of a particular pool over time. Therefore, for tracer studies, such as primary productivity assessments, standard reference materials are necessary only to calibrate instrumentation.

15.5 Editorial note on Chapter 15

When this chapter was written, in 2010-2011 period, named approaches and references were considered state of the art. Current NASA community protocols on Primary Productivity are outlined in IOCCG series report, that is under community review as of February 2022 by *Balch et al.* [2021].

References

Agrawal, Y. C., and H. C. Pottsmith (2000), Instruments for particle size and settling velocity observations in sediment transport, *Marine Geology*, *168*(1), 89-114, doi:https://doi.org/10.1016/S0025-3227(00)00044-X.

Agrawal, Y. C., A. Whitmire, O. A. Mikkelsen, and H. C. Pottsmith (2008), Light scattering by random shaped particles and consequences on measuring suspended sediments by laser diffraction, *Journal of Geophysical Research: Oceans*, *113*(C4), doi:https://doi.org/10.1029/2007JC004403.

Alliet, D. (1975), A study of available particle size standards for calibrating electrical sensing zone methods, *Powder Technol.*, *13*(1), 3-7.

Babin, M., A.Morel, V. Fournier-Sicre, F.Fell, and D. Stramski (2003), Light scattering properties of marine particles in coastal and open waters as related to the particle mass concentration, *Limnology and Oceanography*, *48*(2), 843-859.

Bailey, S. W., S. B. Hooker, D. Antoine, B. A. Franz, and P. J. Werdell (2008), Sources and assumptions for the vicarious calibration of ocean color satellite observations, *Appl. Opt.*, *47*(12), 2035-2045, doi:10.1364/AO.47.002035.

Baker, E. T., and J. W. Lavelle (1984), The effect of particle size on the light attenuation coefficient of natural suspensions, *Journal of Geophysical Research: Oceans*, *89*(C5), 8197-8203, doi:https://doi.org/10.1029/JC089iC05p08197.

Balch, W. M., et al. (2021), Aquatic Primary Productivity Field Protocols for Satellite Validation and Model Synthesis*Rep.*, IOCCG, Dartmouth, NS, Canada.

Balch, W. M., D. T. Drapeau, T. L. Cucci, R. D. Vaillancourt, K. A. Kilpatrick, and J. J. Fritz (1999), Optical backscattering by calcifying algae: Separating the contribution of particulate inorganic and organic carbon fractions, *Journal of Geophysical Research: Oceans*, *104*(C1), 1541-1558, doi:https://doi.org/10.1029/1998JC900035.

Balch, W. M., D. T. Drapeau, J. J. Fritz, B. C. Bowler, and J. Nolan (2001), Optical backscattering in the Arabian Sea--continuous underway measurements of particulate inorganic and organic carbon, *Deep Sea Res Part 1 Oceanogr Res Pap.*, *48*(11), 2423-2452, doi:Doi: 10.1016/s0967-0637(01)00025-5.

Balch, W. M., and V. J. Fabry (2008), Ocean acidification documenting its impact on calcifying phytoplankton at basin scales, *Marine Ecology Progress Series*, *373*, 239-248.

Balch, W. M., H. R. Gordon, B. C. Bowler, D. T. Drapeau, and E. S. Booth (2005), Calcium carbonate measurements in the surface global ocean based on Moderate-Resolution Imaging Spectroradiometer data, *J. Geophys. Res.*, *110*(C7), C07001, doi:10.1029/2004jc002560.

Balch, W. M., P. M. Holligan, S. G. Ackleson, and K. J. Voss (1991), Biological and Optical-Properties of Mesoscale Coccolithophore Blooms in the Gulf of Maine, *Limnology and Oceanography*, *36*(4), 629-643.

Balch, W. M., K. A. Kilpatrick, P. Holligan, D. Harbour, and E. Fernandez (1996), The 1991 coccolithophore bloom in the central North Atlantic .1. Relating optics to coccolith concentration, *Limnology and Oceanography*, *41*(8), 1684-1696.

Balch, W. M., and P. E. Utgoff (2009), POTENTIAL INTERACTIONS AMONG OCEAN ACIDIFICATION, COCCOLITHOPHORES, AND THE OPTICAL PROPERTIES OF SEAWATER, *Oceanography*, *22*(4), 146-159.

Beaufort, L. (2005), Weight Estimates of Coccoliths Using the Optical Properties (Birefringence) of Calcite, *Micropaleontology*, *51*(4), 289-297.

Behrenfeld, M. J., E. Boss, D. A. Siegel, and D. M. Shea (2005), Carbon-based ocean productivity and phytoplankton physiology from space, *Global Biogeochem. Cycles*, *19*(1), GB1006, doi:10.1029/2004GB002299.

Bishop, J. K. B., T.J. Wood, R.E Davis, and J. T. Sherman (2004), Robotic Observations of Enhanced Carbon Biomass and Carbon Export at 55S During SOFeX, *Science*, *304*, 417-420.

Borstad, G. A., E. J. Carpenter, and J. F. R. Gower (1992), Development of Algorithms for Remote Sensing of Trichodesmium Blooms, in *Marine Pelagic Cyanobacteria: Trichodesmium and other Diazotrophs*, edited by E. J. Carpenter, D. G. Capone and J. G. Rueter, pp. 193-210, Springer Netherlands, Dordrecht, doi:10.1007/978-94-015-7977-3_12.

Boss, E., et al. (2019a), IOCCG Ocean Optics and Biogeochemistry Protocols for Satellite Ocean Colour Sensor Validation Inherent Optical Property Measurements and Protocols: Best Practices for the Collection and Processing of Ship-Based Underway Flow-Through Optical Data (v4.0), edited, OCCG Protocol Series, doi:doi:10.25607/OBP-664.

Boss, E., and W. S. Pegau (2001), Relationship of light scattering at an angle in the backward direction to the backscattering coefficient, *Appl. Opt.*, *40*(30), 5503-5507.

Boss, E., W. S. Pegau, M. Lee, M. Twardowski, E. Shybanov, G. Korotaev, and F. Baratange (2004), Particulate backscattering ratio at LEO 15 and its use to study particle composition and distribution, *Journal of Geophysical Research: Oceans*, *109*(C1), n/a-n/a, doi:10.1029/2002jc001514.

Boss, E., et al. (2009), Comparison of inherent optical properties as a surrogate for particulate matter concentration in coastal waters, *Limnol. Oceanogr. Methods*, *7*(11), 803-810, doi:https://doi.org/10.4319/lom.2009.7.803.

Boss, E., M. Twardowski, D. McKee, I. Cetinić, and W. H. Slade (2019b), Beam Transmission and Attenuation Coefficients: Instruments, Characterization, Field Measurements and Data Analysis Protocols*Rep.*, IOCCG, Dartmouth, NS, Canada.

Boutton, T. W., M. J. Lynott, and M. P. Bumsted (1991), Stable carbon isotopes and the study of prehistoric human diet, *Crit. Rev. Food Sci. Nutr.*, *30*(4), 373-385, doi:10.1080/10408399109527548.

Bowers, D. G., and C. E. Binding (2006), The optical properties of mineral suspended particles: A review and synthesis, *Estuar. Coast. Shelf Sci.*, *67*(1), 219-230, doi:https://doi.org/10.1016/j.ecss.2005.11.010.

Boyd, C. M., and G. W. Johnson (1995), Precision of size determination of resistive electronic particle counters, *Journal of plankton research*, *17*(1), 41-58.

Bunt, J. A. C., P. Larcombe, and C. F. Jago (1999), Quantifying the response of optical backscatter devices and transmissometers to variations in suspended particulate matter, *Continental Shelf Research*, *19*(9), 1199-1220, doi:10.1016/s0278-4343(99)00018-7.

Buonassissi, C. J., and H. M. Dierssen (2010), A regional comparison of particle size distributions and the power law approximation in oceanic and estuarine surface waters, *Journal of Geophysical Research: Oceans*, *115*(C10), doi:https://doi.org/10.1029/2010JC006256.

Carpenter, E., A. Subramaniam, and D. Capone (2004), Biomass and primary productivity of the cyanobacterium Trichodesmium spp. in the tropical N Atlantic ocean, *Deep Sea Res Part 1 Oceanogr Res Pap.*, *51*, 173-203, doi:10.1016/j.dsr.2003.10.006.

Chami, M., E. B. Shybanov, G. A. Khomenko, M. E. G. Lee, O. V. Martynov, and G. K. Korotaev (2006), Spectral variation of the volume scattering function measured over the full range of scattering angles in a coastal environment, *Appl. Opt.*, *45*(15), 3605-3619, doi:10.1364/AO.45.003605.

Chaves, J. E., et al. (2021), Particulate Organic Matter Sampling and Measurement Protocols: Consensus Towards Future Ocean Color Missions*Rep.*, IOCCG, Dartmouth, NS, Canada.

Claustre, H., et al. (2004), An intercomparison of HPLC phytoplankton pigment methods using in situ samples: application to remote sensing and database activities, *Marine Chemistry*, *85*(1-2), 41-61, doi:DOI 10.1016/j.marchem.2003.09.002.

Culver, M. E., and M. J. Perry (1997), Calculation of solar-induced fluorescence in surface and subsurface waters, *Journal of Geophysical Research: Oceans*, *102*(C5), 10563-10572.

Dall'Olmo, G., T. K. Westberry, M. J. Behrenfeld, E. Boss, and W. H. Slade (2009), Significant contribution of large particles to optical backscattering in the open ocean, *Biogeosciences*, *6*(6), 947-967.

Fiedler, R., and G. Proksch (1975), The determination of nitrogen-15 by emission and mass spectrometry in biochemical analysis: a review, *Anal. Chim. Acta*, *78*(1), 1-62, doi:https://doi.org/10.1016/S0003-2670(01)84751-6.

Fisher Jr, T. R., E. B. Haines, and R. J. Volk (1979), A comment on the calculation of atom percent enrichment for stable isotopes 1, *Limnology and Oceanography*, *24*(3), 593-595.

Forget, P., S. Ouillon, F. Lahet, and P. Broche (1999), Inversion of reflectance spectra of nonchlorophyllous turbid coastal waters, *Remote Sensing of Environment*, *68*(3), 264-272.

Gardner, W. D., M. J. Richardson, C. A. Carlson, D. Hansell, and A. V. Mishonov (2003), Determining true particulate organic carbon: bottles, pumps and methodologies, *Deep-Sea Res. Part II-Top. Stud. Oceanogr.*, *50*(3-4), 655-674, doi:Pii S0967-0645(02)00589-1.

Gartner, J. W., R. T. Cheng, P. F. Wang, and K. Richter (2001), Laboratory and field evaluations of the LISST-100 instrument for suspended particle size determinations, *Marine Geology*, *175*(1-4), 199-219, doi:10.1016/S0025-3227(01)00137-2.

Gordon, H. R., G. C. Boynton, W. M. Balch, S. B. Groom, D. S. Harbour, and T. J. Smyth (2001), Retrieval of coccolithophore calcite concentration from SeaWiFS Imagery, *Geophys. Res. Lett.*, *28*(8), 1587-1590, doi:10.1029/2000gl012025.

Gordon, H. R., O. B. Brown, R. H. Evans, J. W. Brown, R. C. Smith, K. S. Baker, and D. K. Clark (1988), A semianalytic radiance model of ocean color, *Journal of Geophysical Research: Atmospheres*, *93*(D9), 10909-10924, doi:10.1029/JD093iD09p10909.

Gower, J. (1980), Observations of in situ fluorescence of chlorophyll-a in Saanich Inlet, *Boundary-Layer Meteorology*, *18*, 235-245.

Guay, C. K. H., and J. K. B. Bishop (2002), A rapid birefringence method for measuring suspended CaCO3 concentrations in seawater, *Deep Sea Res Part 1 Oceanogr Res Pap.*, *49*(1), 197-210, doi:https://doi.org/10.1016/S0967-0637(01)00049-8.

Haidar, A. T., and H. R. Thierstein (2001), Coccolithophore dynamics off Bermuda (N. Atlantic), *Deep Sea Research Part II: Topical Studies in Oceanography*, *48*(8), 1925-1956, doi:https://doi.org/10.1016/S0967-0645(00)00169-7.

Hansell, D. A., and C. A. Carlson (1998), Deep-ocean gradients in the concentration of dissolved organic carbon, *Nature*, *395*(6699), 263-266, doi:10.1038/26200.

Hansell, D. A., and C. A. Carlson (2001), Biogeochemistry of total organic carbon and nitrogen in the Sargasso Sea: control by convective overturn, *Deep Sea Research Part II: Topical Studies in Oceanography*, *48*(8), 1649-1667, doi:https://doi.org/10.1016/S0967-0645(00)00153-3.

Hansell, D. A., and E. T. Peltzer (1998), Spatial and temporal variations of total organic carbon in the Arabian Sea, *Deep Sea Research Part II: Topical Studies in Oceanography*, *45*(10), 2171-2193, doi:https://doi.org/10.1016/S0967-0645(98)00067-8.

Hooker, S. B., and J. Aiken (1998), Calibration Evaluation and Radiometric Testing of Field Radiometers with the SeaWiFS Quality Monitor (SQM), *Journal of Atmospheric and Oceanic Technology*, *15*(4), 995-1007, doi:10.1175/1520-0426(1998)015<0995:Cearto>2.0.Co;2.

Hooker, S. B., H. Claustre, J. Ras, L. Van Heukelem, J.-F. Berthon, C. Targa, D. van der Linde, R. Barlow, and H. Sessions (2000), The First SeaWiFS HPLC Analysis Round-Robin Experiment (SeaHARRE-1), in *NASA Tech. Memo. 2000-206892*, edited by S. B. Hooker and E. R. Firestone, p. 42, NASA, Goddard Space Flight Center, Greenbelt, MD.

Hooker, S. B., et al. (2005), The Second SeaWiFS HPLC Analysis Round-Robin Experiment (SeaHARRE-2)*Rep.*, NASA, Goddard Space Fligth Center, Greenbelt, Maryland.

Hooker, S. B., et al. (2010), The Fourth SeaWiFS HPLC Analysis Round-Robin Experiment (SeaHARRE-4)*Rep.*, NASA Goddard Space Flight Center, Greenbelt, Marylan.

Hooker, S. B., G. Lazin, G. Zibordi, and S. McLean (2002a), An Evaluation of Above- and In-Water Methods for Determining Water-Leaving Radiances, *Journal of Atmospheric and Oceanic Technology*, *19*(4), 486-515, doi:10.1175/1520-0426(2002)019<0486:aeoaai>2.0.co;2.

Hooker, S. B., and S. Maritorena (2000), An Evaluation of Oceanographic Radiometers and Deployment Methodologies, *Journal of Atmospheric and Oceanic Technology*, *17*(6), 811-830, doi:10.1175/1520-0426(2000)017<0811:Aeoora>2.0.Co;2.

Hooker, S. B., C. R. McClain, and A. Mannino (2007), NASA Startegic Planning Document: A comprehensive plan for the long-term calibration and validation of oceanic biogeochemical satellite data*Rep. NASA/SP-2007-214152*, NASA.

Hooker, S. B., S. McLean, J. Sherman, M. Small, G. Lazin, G. Zibordi, and J. W. Brown (2002b), The Seventh SeaWiFS Intercalibration Round-Robin Experiment (SIRREX-7), March 1999*Rep.*, 69 pp, Goddard Space Flight Center, Greenbelt, Maryland.

Hooker, S. B., and A. Morel (2003), Platform and environmental effects on above-water determinations of water-leaving radiance, *Journal of Atmospheric and Oceanic Technology*, *20*(1), 187-205.

Hooker, S. B., and L. van Heukelem (2009), CHORS HPLC Uncertainties: Final Report*Rep.*, 62 pp, NASA Goddard Space Flight Center, Greenbelt, Maryland.

Hooker, S. B., and L. van Heukelem (2011), Appendix: a symbology and vocabulary for an HPLC lexicon, in *Phytoplankton Pigments: Characterization, Chemotaxonomy and Applications in Oceanography*, edited by C. A. Llewellyn, E. S. Egeland, G. Johnsen and S. Roy, pp. 195-256, Cambridge University Press, Cambridge, doi:DOI: 10.1017/CBO9780511732263.009.

Hooker, S. B., et al. (2009), The Third SeaWiFS HPLC Analysis Round-Robin Experiment (SeaHARRE-3)*Rep.*, National Aeronautics and Space Administration, Goddard.

Hooker, S. B., and G. Zibordi (2005a), Advanced Methods for Characterizing the Immersion Factor of Irradiance Sensors, *Journal of Atmospheric and Oceanic Technology*, *22*(6), 757-770, doi:10.1175/jtech1736.1.

Hooker, S. B., and G. Zibordi (2005b), Platform perturbations in above-water radiometry, *Appl. Opt.*, *44*(4), 553-567.

Hooker, S. B., G. Zibordi, J.-F. Berthon, and J. W. Brown (2004), Above-water radiometry in shallow coastal waters, *Appl. Opt.*, *43*(21), 4254-4268, doi:10.1364/AO.43.004254.

Hooker, S. B., G. Zibordi, J.-F. Berthon, D. D'Alimonte, S. Maritorena, S. McLean, and J. Sildam (2001), Results of the Second SeaWiFS Data Analysis Round-Robin, March 2000 (DARR-00)*Rep.*, 71 pp, NASA Goddard Space Flight Center, Greenbelt, Maryland.

Huot, Y., C. A. Brown, and J. J. Cullen (2005), New algorithms for MODIS sun-induced chlorophyll fluorescence and a comparison with present data products, *Limnology and Oceanography-Methods*, *3*, 108-130.

Hynes, A. M. (2009), Diversity of the Marine Cyanobacterium Trichodesmium: Characterization of the Woods Hole Culture Collection and Quantification of Field Populations, MIT/Woods Hole Oceanographic Institution.

Johnson, B. C., S. W. Brown, K. R. Lykke, C. E. Gibson, G. Fargion, G. Meister, S. B. Hooker, B. Markham, and J. J. Butler (2003), Comparison of cryogenic radiometry and thermal radiometry calibrations at NIST using multichannel filter radiometers, *Metrologia*, *40*(1), S216.

Johnson, B. C., H. W. Yoon, S. S. Bruce, P.-S. Shaw, A. Thompson, S. B. Hooker, J. R.E. Eplee, R. A. Barnes, S. Maritorena, and J. L. Mueller (1999), The fifth SeaWiFS intercalibration round-robin experiment (SIRREX-5), July 1996*Rep.*, Goddard Space Flight Center, Greenbelt, Maryland.

Kadar, S., M. Leinen, and J. W. Murray (1993), Sampling and Analytical Protocols for the Joint Global Ocean Flux Study (JGOFS) Equatorial Pacific Process Study.

Kiefer, D. A., W. S. Chamberlin, and C. R. Booth (1989), Natural fluorescence of chlorophyll a: Relationship to photosynthesis and chlorophyll concentration in the western South Pacific gyre, *Limnology and Oceanography*, *34*(5), 868-881.

Kirk, J. (1992), Monte Carlo modeling of the performance of a reflective tube absorption meter, *Appl. Opt.*, *31*(30), 6463-6468.

Kirk, J. T. O. (1994), *Light and photosynthesis in aquatic environments*, Cambridge University Press.

Knap, A., A. Michaels, A. Close, H. Ducklow, and A. Dickson (Eds.) (1996), *Protocols for the Joint Global Ocean Flux studies (JGOFS) core measurements (JGOFS Report Nr. 19)*, Reprint of the IOC Manuals and Guides No. 29, UNESCO 1994 ed., vi+170 pp pp., UNESCO, Paris.

Kostadinov, T. S., D. A. Siegel, and S. Maritorena (2009), Retrieval of the particle size distribution from satellite ocean color observations, *J. Geophys. Res.*, *114*, doi:10.1029/2009jc005303.

Kovesi, P. (1999), Phase preserving denoising of images, paper presented at DICTA'99 Digital Image Computing: Techniques & Applications, APRS Perth, Australia.

Leathers, R. A., T. V. Downes, and C. O. Davis (2000), Analysis of a point-source integrating-cavity absorption meter, *Appl. Opt.*, *39*(33), 6118-6127, doi:10.1364/AO.39.006118.

Letelier, R. M., and M. R. Abbott (1996), An analysis of chlorophyll fluorescence algorithms for the Moderate Resolution Imaging Spectrometer (MODIS), *Remote Sensing of the Environment*, *58*, 215-223.

Letelier, R. M., and D. M. Karl (1996), Role of Trichodesmium spp. in the productivity of the subtropical North Pacific Ocean, *Marine Ecology Progress Series*, *133*, 263-273.

Maffione, R. A., and D. R. Dana (1997), Instruments and methods for measuring the backward-scattering coefficient of ocean waters, *Appl. Opt.*, *36*(24), 6057-6067.

Mannino, A., et al. (2019), Measurement protocol of absorption by chromophoric dissolved organic matter (CDOM) and other dissolved materials*Rep.*

Meister, G., et al. (2002), The First SIMBIOS Radiometric Intercomparison (SIMRIC-1), April–September 2001*Rep.*, 60 pp, Goddard Space Flight Center, Greenbelt, Maryland.

Mikkelsen, O. A., P. S. Hill, T. G. Milligan, and R. J. Chant (2005), In situ particle size distributions and volume concentrations from a LISST-100 laser particle sizer and a digital floc camera, *Continental Shelf Research*, *25*(16), 1959-1978, doi:https://doi.org/10.1016/j.csr.2005.07.001.

Milligan, T. G., and K. Kranck (1991), Electroresistance particle size analyzers, in *Principles, Methods, and Application of Particle Size Analysis*, edited by J. Syvitski, pp. 109-118, Cambridge Univ. Press, Cambridge, U.K.

Mitchell, B. G., et al. (2000), Determination of spectral absorption coefficients of particles, dissolved material and phytoplankton for discrete water samples*Rep.*, 125-153 pp.

Mitchell, B. G., M. Kahru, J. Wieland, and M. Stramska (2002), Determination of spectral absorption coefficients of particles, dissolved material and phytoplankton for discrete water samples*Rep.*, 39-67 pp, National Aeronautics and Space Administration, Greenbelt, MD.

Montoya, J. P., M. Voss, P. Kahler, and D. G. Capone (1996), A simple, high-precision, high-sensitivity tracer assay for N (inf2) fixation, *Applied and environmental microbiology*, *62*(3), 986-993.

Morel, A., and B. Gentili (2004), Radiation transport within oceanic (case 1) water, *Journal of Geophysical Research-Oceans*, *109*(C6), C06008, doi:10.1029/2003jc002259.

Morel, A., and R. C. Smith (1974), Relation between total quanta and total energy for aquatic photosynthesis1, *Limnology and Oceanography*, *19*(4), 591-600, doi:https://doi.org/10.4319/lo.1974.19.4.0591.

Mueller, J. L., et al. (2003), Radiometric measurements and data analysis protocols*Rep.*, NASA, Goddard Space Flight Center, Greenbelt, MD.

Mulholland, M. R., P. W. Bernhardt, C. A. Heil, D. A. Bronk, and J. M. O'Neil (2006), Nitrogen fixation and release of fixed nitrogen by Trichodesmium spp. in the Gulf of Mexico, *Limnology and Oceanography*, *51*(4), 1762-1776.

Mulholland, M. R., G. E. Boneillo, P. W. Bernhardt, and E. C. Minor (2009), Comparison of nutrient and microbial dynamics over a seasonal cycle in a mid-Atlantic coastal lagoon prone to Aureococcus anophagefferens (brown tide) blooms, *Estuar Coasts*, *32*(6), 1176-1194.

Neeley, A. R., and A. Mannino (2018), Ocean Optics and Biogeochemistry Protocols for Satellite Ocean Colour Sensor Validation; Volume 1.0. Inherent Optical Property Measurements and Protocols: Absorption Coefficient.

Neeley, A. R., C. S. Thomas, S. B. Hooker, and L. van Heukelem (2011), Appendix B. The pigment analyst's guide to HPLC hardware, in *Phytoplankton Pigments: Characterization, Chemotaxonomy and Applications in Oceanography*, edited by C. A. Llewellyn, E. S. Egeland, G. Johnsen and S. Roy, pp. 195-256, Cambridge University Press, Cambridge, doi:DOI: 10.1017/CBO9780511732263.009.

Norrman, B. (1993), Filtration of water samples for DOC studies, *Marine Chemistry*, *41*(1), 239-242, doi:https://doi.org/10.1016/0304-4203(93)90125-8.

Parsons, T. R., Y. Maita, and C. M. Lalli (1984), *A Manual of Chemical and Biological Methods for Seawater Analysis*, 173 pp., Pergamon Press, Oxford, UK.

Pegau, S., J. R. V. Zaneveld, B. G. Mitchell, J. L. Mueller, M. Kahru, J. Wieland, and M. Stramska (2003), Inherent Optical Properties: Instruments, Characterizations, Field Measurements and Data Analysis Protocols*Rep.*, NASA, Goddard Space Flight Center, Greenbelt, MD.

Preisendorfer, R. W. (1976), Hydrologic Optics. Volume 5. Properties*Rep.*, Honolulu: US Dept. of Commerce, National Oceanic and Atmospheric ….

Ruddick, K. G., V. De Cauwer, Y.-J. Park, and G. Moore (2006), Seaborne measurements of near infrared water-leaving reflectance: The similarity spectrum for turbid waters, *Limnology and Oceanography*, *51*(2), 1167-1179.

Sakshaug, E., A. Bricaud, Y. Dandonneau, P. G. Falkowski, D. A. Kiefer, L. Legendre, A. Morel, J. Parslow, and M. Takahashi (1997), Parameters of photosynthesis: definitions, theory and interpertation of results, *Journal of Plankton Research*, *19*(11), 1637-1670.

Shang, S., Z. Lee, and G. Wei (2011), Characterization of MODIS-derived euphotic zone depth: Results for the China Sea, *Remote Sensing of Environment*, *115*(1), 180-186.

Sharp, J. H., R. Benner, L. Bennett, C. A. Carlson, S. E. Fitzwater, E. T. Peltzer, and L. M. Tupas (1995), Analyses of dissolved organic carbon in seawater: the JGOFS EqPac methods comparison, *Marine Chemistry*, *48*(2), 91-108, doi:https://doi.org/10.1016/0304-4203(94)00040-K.

Sharp, J. H., C. A. Carlson, E. T. Peltzer, D. M. Castle-Ward, K. B. Savidge, and K. R. Rinker (2002), Final dissolved organic carbon broad community intercalibration and preliminary use of DOC reference materials, *Marine Chemistry*, *77*(4), 239-253, doi:https://doi.org/10.1016/S0304-4203(02)00002-6.

Sharp, J. H., et al. (1993), Procedures subgroup report, *Marine Chemistry*, *41*(1), 37-49, doi:https://doi.org/10.1016/0304-4203(93)90104-V.

Sherr, E. B., D. A. Caron, and B. F. Sherr (1993), Staining of heterotrophic protists for visualization via epifluorescence microscopy, in *Handbook of methods in aquatic microbial ecology*, edited, pp. 213-227, CRC press.

Siegel, D., M. O'Brien, J. Sorensen, D. Konnoff, E. Brody, J. Mueller, C. Davis, W. Rhea, and S. Hooker (1995), Results of the SeaWiFS Data Analysis Round-Robin (DARR-94), July 1994*Rep.*, 58 pp, NASA Goddard Space Flight Center, Greenbelt, Maryland.

Slade, W. H., and E. S. Boss (2006), Calibrated near-forward volume scattering function obtained from the LISST particle sizer, *Opt. Express*, *14*(8), 3602-3615, doi:10.1364/OE.14.003602.

Slawyk, G., Y. Collos, and J. C. Auclair (1977), The use of the 13C and 15N isotopes for the simultaneous measurement of carbon and nitrogen turnover rates in marine phytoplankton 1, *Limnology and Oceanography*, *22*(5), 925-932.

Stramski, D., E. Boss, D. Bogucki, and K. J. Voss (2004), The role of seawater constituents in light backscattering in the ocean, *Progress in Oceanography*, *61*(1), 27-56.

Stramski, D., et al. (2008), Relationships between the surface concentration of particulate organic carbon and optical properties in the eastern South Pacific and eastern Atlantic Oceans, *Biogeosciences*, *5*(1), 171-201, doi:10.5194/bg-5-171-2008.

Stumpf, R. P. (1988), Sediment Transport in Chesapeake Bay during Floods: Analysis Using Satellite and Surface Observations, *Journal of Coastal Research*, *4*(1), 1-15.

Subramaniam, A., C. W. Brown, R. R. Hood, E. J. Carpenter, and D. G. Capone (2001), Detecting Trichodesmium blooms in SeaWiFS imagery, *Deep Sea Research Part II: Topical Studies in Oceanography*, *49*(1-3), 107-121.

Sullivan, J. M., and M. S. Twardowski (2009), Angular shape of the oceanic particulate volume scattering function in the backward direction, *Appl. Opt.*, *48*(35), 6811-6819.

Traykovski, P., R. J. Latter, and J. D. Irish (1999), A laboratory evaluation of the laser in situ scattering and transmissometery instrument using natural sediments, *Marine Geology*, *159*(1-4), 355-367.

Tupas, L. M., B. N. Popp, and D. M. Karl (1994), Dissolved organic carbon in oligotrophic waters: experiments on sample preservation, storage and analysis, *Marine Chemistry*, *45*(3), 207-216, doi:https://doi.org/10.1016/0304-4203(94)90004-3.

Twardowski, M. S., H. Claustre, S. A. Freeman, D. Stramski, and Y. Huot (2007), Optical backscattering properties of the "clearest" natural waters, *Biogeosciences*, *4*, 1041-1058.

Tyler, J. E. (1966), *Report of the second meeting of the joint group of experts on photosynthetic radiant energy / jointly sponsored by the United Nations Educational, Scientific and Cultural Organization, Scientific Committee on Oceanic Research, International Association of Physical Oceanography (Karuizawa, 15-19 August, 1966)*, Unesco, Paris.

van Heukelem, L., and S. B. Hooker (2011), The importance of a quality assurance plan for method validation and minimizing uncertainties in the HPLC analysis of phytoplankton pigments, in *Phytoplankton Pigments: Characterization, Chemotaxonomy and Applications in Oceanography*, edited by C. A. Llewellyn, E. S. Egeland, G. Johnsen and S. Roy, pp. 195-256, Cambridge University Press, Cambridge, doi:DOI: 10.1017/CBO9780511732263.009.

Van Heukelem, L., and C. S. Thomas (2001), Computer-assisted high-performance liquid chromatography method development with applications to the isolation and analysis of phytoplankton pigments, *Journal of Chromatography A*, *910*(1), 31-49.

Vuorio, K., L. Lepistoe, and A. L. Holopainen (2007), Intercalibrations of freshwater phytoplankton analyses, *Boreal Environment Research*, *12*, 561-569.

Westberry, T., D. A. Siegel, and A. Subramaniam (2005), An improved bio-optical model for the remote sensing of Trichodesmium spp. blooms, *Journal of Geophysical Research: Oceans*, *110*(C6), doi:10.1029/2004JC002517.

Woodruff, D. L., R. P. Stumpf, J. A. Scope, and H. W. Paerl (1999), Remote estimation of water clarity in optically complex estuarine waters, *Remote sensing of Environment*, *68*(1), 41-52.

Zhang, X., L. Hu, and M.-X. He (2009), Scattering by pure seawater: Effect of salinity, *Opt. Express*, *17*(7), 5698-5710.

Zibordi, G., S. B. Hooker, J. Mueller, and G. Lazin (2004), Characterization of the Immersion Factor for a Series of In-Water Optical Radiometers, *Journal of Atmospheric and Oceanic Technology*, *21*(3), 501-514, doi:10.1175/1520-0426(2004)021<0501:Cotiff>2.0.Co;2.

Zibordi, G., K. J. Voss, B. C. Johnson, and J. Mueller (2019), Protocols for Satellite Ocean Colour Sensor Validation*Rep.*, IOCCG, Dartmouth, NS, Canada.

Previous Volumes in This Series

Volume 1 *April 2018*	ACE Ocean Working Group recommendations and instrument requirements for an advanced ocean ecology mission
Volume 2 *May 2018*	Pre-Aerosol, Clouds, and ocean Ecosystem (PACE) Mission Science Definition Team Report
Volume 3 *October 2018*	Polarimetry in the PACE mission: Science Team consensus document
Volume 4 *October 2018*	Cloud retrievals in the PACE mission: Science Team consensus document
Volume 5 *December 2018*	Mission Formulation Studies
Volume 6 *December 2018*	Data Product Requirements and Error Budgets
Volume 7 *December 2018*	Ocean Color Instrument (OCI) Concept Design Studies
Volume 8 *September 2020*	The PACE Science Data Product Selection Plan
Volume 9 *October 2020*	PACE Application Plan